NUMERICAL STUDY OF A QUANTUM-DIFFUSIVE SPIN MODEL FOR TWO-DIMENSIONAL ELECTRON GASES

LUIGI BARLETTI, FLORIAN MÉHATS, CLAUDIA NEGULESCU,
AND STEFAN POSSANNER

December 13, 2012

Abstract. We investigate the time evolution of spin densities in a two-dimensional electron gas subjected to Rashba spin-orbit coupling on the basis of the quantum drift-diffusive model derived in Ref. [2]. This model assumes the electrons to be in a quantum equilibrium state in the form of a Maxwellian operator. The resulting quantum drift-diffusion equations for spin-up and spin-down densities are coupled in a non-local manner via two spin chemical potentials (Lagrange multipliers) and via off-diagonal elements of the equilibrium spin density and spin current matrices, respectively. We present two space-time discretizations of the model which comprise also the Poisson equation in order to account for electron-electron interactions. In a first step pure time discretization is applied in order to prove the well-posedness of the two schemes, both of which are based on a functional formalism to treat the non-local relations between spin densities. We then use the fully space-time discrete schemes to simulate the time evolution of a Rashba electron gas in a typical transistor geometry. Finite difference approximations are first order in time and second order in space. The discrete functionals introduced are minimized with the help of a conjugate gradient-based algorithm, where the Newton method is applied in order to find the respective line minima.

1. Introduction

The purpose of this paper is the numerical study of the quantum diffusive model for a spin-orbit system introduced in Ref. [2], with the aim of developing numerical tools for the investigation of spin-based electronic devices.

Diffusive models offer a simple, yet fairly accurate, description of charge transport and, for this reason, they have a long-standing tradition in semiconductor modeling. Classical drift-diffusion equations for semiconductors [12] were first derived by van Roosbroeck [17], while Poupaud [16] proved their rigorous derivation from the Boltzmann equation. Quantum-corrected drift-diffusion equations were proposed in Refs. [1, 7], and were later derived by using a quantum version of the maximum entropy principle by Degond, Méhats and Ringhofer [5, 6]. Finally, fully-quantum diffusive equations, still

based on the quantum maximum entropy principle, were proposed in Refs. [4, 5]. In view of recent progresses in controlling the electron spin, it is highly desirable to extend the drift-diffusion description to the spinorial case. The existing semiclassical drift-diffusion models for spin systems can be classified into two categories: the two-component models [9] and the spin-polarized or matrix models [9, 15, 18]. Both models have been used in practice, however their mathematical derivation is still at the very beginning.

As far as we know, a fully-quantum diffusive model of a spin system has been first reported in Ref. [2], where a two-component diffusive model for a 2-dimensional electrons gas with spin-orbit interaction is derived. Such model, which will be considered from the numerical point of view in the present work, is based on the quantum maximum entropy principle and concerns electrons with a spin-orbit Hamiltonian of Rashba type [3]:

$$H = \begin{pmatrix} -\frac{\hbar^2}{2}\,\Delta + V & \alpha\hbar(\partial_x - i\partial_y) \\ -\alpha\hbar(\partial_x + i\partial_y) & -\frac{\hbar^2}{2}\,\Delta + V \end{pmatrix}. \tag{1}$$

Here, (x, y) are the spatial coordinates of the 2-dimensional region where the electrons are assumed to be confined, α is the Rashba constant and V is a potential term which may consist of an "external" part (representing e.g. a gate or an applied potential) and a self-consistent part, accounting for Coulomb interactions in the mean-field approximation.

The Rashba effect [3, 19] is a spin-orbit interaction undergone by electrons that are confined in an asymmetric 2-dimensional well (here, perpendicular to the z direction). Due to this interaction, the spin vector has a precession around a direction in the plane (x, y), perpendicular to the electron momentum $p = (p_x, p_y)$, the precession speed being $\alpha|p|$. Since it does not involve built-in magnetic fields, and hence may be implemented by means of standard silicon technologies, the Rashba effect is expected to be a key ingredient for the realization of the so-called S-FET (Spin Field Effect Transistor) [19], a "spintronic" device in which the information is carried by the electron spin rather than by the electronic current (as in the usual electronic devices). This may lead to electronic devices of higher speed and lower power consumption. The purpose of this work is to contribute to the understanding of how the Rashba effect can be employed in order to control the spin transport in these devices.

Let us summarize briefly the derivation of the here investigated quantum diffusive model. The starting point is the von Neumann equation (i.e. the Schrödinger equation for mixed states) for the Hamiltonian (1), endowed with a collisional term of BGK type

$$i\hbar\partial_t \varrho(t) = [H, \varrho(t)] + \frac{i}{\tau}\left(\varrho_{eq} - \varrho(t)\right),$$

where $\varrho(t) = (\varrho_{ij}(t))$ is the 2×2 density operator, representing the time-dependent mixed state of the system, and τ is the relaxation time. According to the theory developed in Refs. [6, 5] , the local equilibrium state ϱ_{eq} is chosen as the maximizer of a free energy-like functional, subject to the constraint of sharing with $\varrho(t)$ the local moments we are interested in, here the spin-up and spin-down (with respect to the z direction) electron densities n_1, n_2 (or, equivalently, the total electronic density $n_1 + n_2$ and the polarization $n_1 - n_2$). Then, the maximizer, which has the form of a Maxwellian operator, contains as many Lagrange multipliers (chemical potentials) as the chosen moments. These multipliers furnish the degrees of freedom necessary to satisfy the constraint equations. In our case, therefore, the local equilibrium state contains two chemical potential, A_1 and A_2, which depend on n_1 and n_2 through the constraint equations. The rigorous proof of realizability of the quantum Maxwellian associated to a given density and current has been obtained in Refs. [13, 14] for a scalar (i.e. non spinorial) Hamiltonian. By assuming $\tau \ll 1$ and applying the Chapman-Enskog method, the von Neumann equation leads in the limit to the "quantum drift-diffusive" system (2) for the unknown densities n_1 and n_2. Apart from the chemical potentials A_1 and A_2, which depend on n_1 and n_2 through the constraint, the system also contains some extra moments, namely the off-diagonal density n_{21} and currents J^x_{21}, J^y_{21}, which are computed via the equilibrium state and which depend on n_1 and n_2 as well. Note that, with respect to the original Hamiltonian (1), we shall work with a scaled version (see the Hamiltonian (5), which contains also the chemical potential) in which ε is the scaled Planck constant and α is rescaled as $\varepsilon\alpha$. This is, therefore, a semiclassical scaling with the additional assumption of small Rashba constant. Of course, the parameter ε is unimportant as long as we are not interested in the semiclassical behavior but becomes relevant when we look for a semiclassical expansion of the model for small ε.

In summary, the diffusive equations (2), coupled to Eqs. (4)–(8) which represent the equilibrium state and the constraints, and associated with the Poisson equation (3) for the self-consistent potential, constitute the quantum diffusive model we are going to analyze numerically in this work. Needless to say, the model (2)–(8) is rather implicit and involved, and requires a very careful numerical treatment. The aim of the present paper is thus to present two discrete versions of (2)–(8), suitable for time-resolved simulation of the spin densities n_1 and n_2 in a spatially confined, two-dimensional electron gas. In both schemes the finite-difference approximations of the occurring derivatives are first order in time and second order in space. At the core of the numerical study of the present model is the minimization of a functional

that either maps from $\mathbb{R}^{3P}$ to $\mathbb{R}$ (in the first scheme) or from $\mathbb{R}^{2P}$ to $\mathbb{R}$ (in the second scheme), where P is the number of points on the space grid. We present an algorithm that uses a combination of the conjugate gradient method and the Newton method in order to find the minimum of the respective functional at each time step. The developed numerical schemes are used to compute the equilibrium spin densities in a common transistor geometry which features a spin-dependent potential barrier.

The paper is organized as follows. In Section 2, the continuous model is introduced and is endowed with suitable initial and boundary conditions. In Sec. 3 we perform two different time discretizations of the continuous model and give a formal proof of the well-posedness of each of the two schemes. Then, in Sec. 4 two fully discrete schemes (i.e. both in time and space) are introduced and analyzed as well. Finally, Sec. 5 is devoted to numerical experiments. Details of the proofs and of the discretization matrices are deferred to the appendices.

2. The quantum spin drift-diffusion model

Let us start with the presentation of the quantum diffusive model introduced in Ref. [2]. The model describes the evolution of the spin-up and the spin-down densities n_1 and n_2, respectively, of a two-dimensional electron gas by means of the following quantum drift-diffusion equations:

$$\begin{aligned}
&\partial_t n_1 + \nabla\cdot(n_1\nabla(A_1-V_s))+\\
&\qquad +\alpha(A_1-A_2)\,\mathcal{R}\mathrm{e}(\mathcal{D}n_{21}) - 2\alpha\,\mathcal{R}\mathrm{e}(n_{21}\mathcal{D}(A_2-V_s))-\\
&\qquad -\frac{2\alpha}{\varepsilon}(A_1-A_2)\,\mathcal{I}\mathrm{m}(J^x_{21}-iJ^y_{21}) = 0\,,\\
&\partial_t n_2 + \nabla\cdot(n_2\nabla(A_2-V_s))+\\
&\qquad +\alpha(A_1-A_2)\,\mathcal{R}\mathrm{e}(\mathcal{D}n_{21}) + 2\alpha\,\mathcal{R}\mathrm{e}(n_{21}\mathcal{D}(A_1-V_s))+\\
&\qquad +\frac{2\alpha}{\varepsilon}(A_1-A_2)\,\mathcal{I}\mathrm{m}(J^x_{21}-iJ^y_{21}) = 0\,.
\end{aligned} \tag{2}$$

Here, $\nabla = (\partial_x, \partial_y)$, $\mathcal{D} = \partial_x - i\partial_y$, A_1 and A_2 denote the two Lagrange multipliers ($A_1 - V_s$ and $A_2 - V_s$ being the chemical potentials), V_s stands for the self-consistent potential arising from the electron-electron interaction and n_{21}, J^x_{21} and J^y_{21} are off-diagonal elements of the spin-density matrix N and the spin-current tensor J written in (7) and (8), respectively. The parameter $\alpha > 0$ denotes the scaled Rashba constant and $\varepsilon > 0$ stands for the scaled Planck constant (for details regarding the scaling we refer to [2]). The self-consistent potential V_s is determined by the Poisson equation,

$$-\gamma^2\Delta V_s = n_1 + n_2\,, \tag{3}$$

where $\gamma > 0$ is proportional to the occurring Debye length. The system (2)-(3) is closed through the fact that the electrons are assumed to be in a quantum local equilibrium state at all times. This constraint allows one to relate the Lagrange multipliers $A = (A_1, A_2)$ to the spin densities n_1 and n_2 as well as to the spin-mixing quantities n_{21} and J_{21}, respectively. More precisely, if $H(A)$ denotes the system Hamiltonian, the equilibrium state operator is given by

$$\varrho_{eq} = \exp(-H(A)), \tag{4}$$

where $\exp(\cdot)$ here denotes the operator exponential. In the present case, the Hamiltonian is given by

$$\begin{aligned} H(A) &: D(H) \subset (L^2(\Omega))^2 \to (L^2(\Omega))^2\,, \quad D(H) \subset (H^2(\Omega))^2\,, \\ H(A) &= \begin{pmatrix} -\frac{\varepsilon^2}{2}\,\Delta + V_{ext,1} + A_1 & \varepsilon^2\alpha(\partial_x - i\partial_y) \\ -\varepsilon^2\alpha(\partial_x + i\partial_y) & -\frac{\varepsilon^2}{2}\,\Delta + V_{ext,2} + A_2 \end{pmatrix}, \end{aligned} \tag{5}$$

where $\Omega \subset \mathbb{R}^2$ denotes the bounded domain where the electrons are assumed to be confined. Moreover, we introduced two external, time-independent potentials $V_{ext,1}(x)$ and $V_{ext,2}(x)$ for the spin-up and the spin-down electrons, respectively. Assuming that $H(A)$ has a pure point spectrum, the eigenvalues and the eigenvectors of $H(A)$, denoted by $\lambda_l(A)$ and $\psi_l(A) = (\psi_l^1(A), \psi_l^2(A))$, $l \in \mathbb{N}$, respectively, are solutions of

$$H(A)\psi_l(A) = \lambda_l(A)\psi_l(A)\,, \tag{6}$$

and link the Lagrange multipliers to the spin-density matrix N as well as to the spin-current matrix J, according to

$$N = \sum_l e^{-\lambda_l} \begin{pmatrix} |\psi_l^1|^2 & \psi_l^1\,\overline{\psi_l^2} \\ \psi_l^2\,\overline{\psi_l^1} & |\psi_l^2|^2 \end{pmatrix} = \begin{pmatrix} n_1 & \overline{n}_{21} \\ n_{21} & n_2 \end{pmatrix}, \tag{7}$$

$$\begin{aligned} J &= -\frac{i\varepsilon}{2} \sum_l e^{-\lambda_l} \begin{pmatrix} \overline{\psi_l^1}\nabla\psi_l^1 - \psi_l^1\nabla\overline{\psi_l^1} & \overline{\psi_l^2}\nabla\psi_l^1 - \psi_l^1\nabla\overline{\psi_l^2} \\ \overline{\psi_l^1}\nabla\psi_l^2 - \psi_l^2\nabla\overline{\psi_l^1} & \overline{\psi_l^2}\nabla\psi_l^2 - \psi_l^2\nabla\overline{\psi_l^2} \end{pmatrix} \\ &= \begin{pmatrix} J_1 & \overline{J}_{21} \\ J_{21} & J_2 \end{pmatrix}. \end{aligned} \tag{8}$$

The formulas (7) and (8) are the standard textbook expressions for the spin-density and the spin-current, respectively, corresponding to the density operator (4). The system (2)-(3) is now closed through the non-local relations $N(A)$ and $J(A)$, given by Eqs. (5)-(8). As we do not have a proof of the invertibility of these relations, in other words whether it is possible to compute $A(n_1, n_2)$, the equations (2) can also be viewed as evolution equations for the Lagrange multipliers A_1 and A_2 rather than for the spin densities n_1 and n_2. Indeed, the two time-discretizations of the system

(2)-(8), which will be developed in section 3, represent these two possible viewpoints regarding the evolution equations (2).

Let us now come to the boundary conditions of our problem. The considered spatial domain $\Omega \subset \mathbb{R}^2$ is assumed to be bounded with regular boundary $\partial\Omega$. We shall impose Dirichlet boundary conditions for the eigenvectors ψ_l,

$$\psi_l(x) = 0 \quad \text{for} \quad x \in \partial\Omega\,,$$

hence the current across the domain boundary $\partial\Omega$ is zero. As we will briefly show at the end of this section, the Hamiltonian (5) is not hermitian in $(L^2(\Omega))^2$ when imposing Neumann conditions on the wavefunctions $\psi \in (H^2(\Omega))^2$. The study of this problem as well as the implementation of transparent boundary conditions can be matter for a future work. The self-consistent potential V_s is supplemented with Dirichlet conditions too,

$$V_s(x) = 0 \quad \text{for} \quad x \in \partial\Omega\,.$$

The Lagrange multipliers A_1 and A_2 are allowed to vary freely at the boundary, therefore we take Neumann conditions,

$$\nabla(A_1(x) - V_s(x)) \cdot \nu(x) = 0 \quad \text{for} \quad x \in \partial\Omega\,,$$
$$\nabla(A_2(x) - V_s(x)) \cdot \nu(x) = 0 \quad \text{for} \quad x \in \partial\Omega\,.$$

Here, $\nu(x)$ denotes the outward normal to the boundary $\partial\Omega$ at x. As far as initial conditions are concerned, one has two choices depending on the point of view of the evolution equations (2). Since we do not know whether or not (7) is invertible, the safe approach is to provide initial data for the chemical potentials. However, from the viewpoint of device modeling, it is more appealing to start from initial spin densities. We shall take the latter approach and assume that $n_1(0,x)$ and $n_2(0,x)$ are smooth and bounded.

In summary, we have the following quantum spin-drift-diffusion model,

$$\partial_t n_1 + \nabla \cdot (n_1 \nabla(A_1 - V_s)) + \alpha(A_1 - A_2)\,\mathcal{R}\mathrm{e}(\mathcal{D} n_{21}) \qquad (9)$$
$$- 2\alpha\,\mathcal{R}\mathrm{e}(n_{21}\mathcal{D}(A_2 - V_s)) - \frac{2\alpha}{\varepsilon}(A_1 - A_2)\,\mathcal{I}\mathrm{m}(J^x_{21} - iJ^y_{21}) = 0\,,$$

$$\partial_t n_2 + \nabla \cdot (n_2 \nabla(A_2 - V_s)) + \alpha(A_1 - A_2)\,\mathcal{R}\mathrm{e}(\mathcal{D} n_{21}) \qquad (10)$$
$$+ 2\alpha\,\mathcal{R}\mathrm{e}(n_{21}\mathcal{D}(A_1 - V_s)) + \frac{2\alpha}{\varepsilon}(A_1 - A_2)\,\mathcal{I}\mathrm{m}(J^x_{21} - iJ^y_{21}) = 0\,,$$

$$-\gamma^2 \Delta V_s = n_1 + n_2\,, \qquad (11)$$

$$H(A)\psi_l(A) = \lambda_l(A)\psi_l(A)\,, \qquad (12)$$

$$N = \sum_l e^{-\lambda_l(A)} \begin{pmatrix} |\psi_l^1(A)|^2 & \psi_l^1(A)\,\overline{\psi_l^2}(A) \\ \psi_l^2(A)\,\overline{\psi_l^1}(A) & |\psi_l^2(A)|^2 \end{pmatrix}, \tag{13}$$

$$J_{21} = -\frac{i\varepsilon}{2} \sum_l e^{-\lambda_l(A)} \left(\overline{\psi_l^1}(A) \nabla \psi_l^2(A) - \psi_l^2(A) \nabla \overline{\psi_l^1}(A) \right), \tag{14}$$

where the Hamiltonian $H(A)$ is given by (5), and supplemented with the following initial and boundary conditions,

$$\begin{aligned} &n_1(t=0,x) = n_1^0(x)\,, \quad n_2(t=0,x) = n_2^0(x) \quad \text{for} \quad x \in \Omega\,, \\ &V_s(x) = 0 \quad \text{for} \quad x \in \partial\Omega\,, \\ &\psi_l(x) = 0 \quad \text{for} \quad x \in \partial\Omega\,, \\ &\nabla(A_1(x) - V_s(x)) \cdot \nu(x) = 0 \quad \text{for} \quad x \in \partial\Omega\,, \\ &\nabla(A_2(x) - V_s(x)) \cdot \nu(x) = 0 \quad \text{for} \quad x \in \partial\Omega\,. \end{aligned} \tag{15}$$

Let us finish this section, by remarking that the Hamiltonian (5) is not hermitian in $(L^2(\Omega))^2$ when imposing Neumann boundary conditions on the wave functions $\psi \in (H^2(\Omega))^2$. Indeed, let us consider

$$(H(A)\psi, \chi) = \int_\Omega (\overline{\chi^1}, \overline{\chi^2}) \begin{pmatrix} -\frac{\varepsilon^2}{2}\,\Delta\psi^1 + (V_{ext,1} + A_1)\psi^1 + \varepsilon^2 \alpha \mathcal{D}\psi^2 \\ -\frac{\varepsilon^2}{2}\,\Delta\psi^2 + (V_{ext,2} + A_2)\psi^2 - \varepsilon^2 \alpha \mathcal{D}\psi^1 \end{pmatrix} dx\,,$$

where $(\cdot,\cdot)$ denotes here the scalar product in $(L^2(\Omega))^2$. Specifically, let us look at the Rashba coupling terms,

$$\begin{aligned} \int_\Omega (\overline{\chi^1}\mathcal{D}\psi^2 - \overline{\chi^2}\mathcal{D}\psi^1)\,dx = &- \int_\Omega (\psi^2 \mathcal{D}\overline{\chi^1} - \psi^1 \mathcal{D}\overline{\chi^2})\,dx + \\ &+ \int_{\partial\Omega} \overline{\chi^1}\psi^2(1,-i)\cdot\nu(x)\,d\sigma - \int_{\partial\Omega} \overline{\chi^2}\psi^1(1,-i)\cdot\nu(x)\,d\sigma\,. \end{aligned} \tag{16}$$

Here, the boundary terms do not vanish when imposing Neumann conditions. However, if we considered the problem in the whole space $\Omega = \mathbb{R}^2$, the boundary terms would vanish and the Hamiltonian would be hermitian. Considering the problem in the whole $\mathbb{R}^2$ means, from the numerical point of view, imposing transparent boundary conditions for ψ.

3. Semi-discretization in time

In this section we make a first step towards a full space-time discretization of the system (9)-(15), by discretizing the time domain. The purpose of the semi-discretization is two-fold. Firstly, since the space discretization of the present two-dimensional spin model is quite involved, the functional formalism which will be applied in this work becomes more transparent in the semi-discrete case than in the fully discrete case. Secondly, in contrast

to the continuous case (9)-(15), existence and uniqueness of solutions of the semi-discrete system can be proven. Two different semi-discretizations will be presented. The first one was studied in [8] for a scalar quantum diffusive model (without the Rashba spin-orbit coupling). We shall use some of the techniques elaborated in [8] and apply them to the present spin model. The second semi-discrete scheme is an explicit one which relies heavily on the ability to invert the relation (13). Its benefits lie in the fact that, when passing to the full discretization, its treatment is far less involved as compared to the first scheme.

In the subsequent analysis, the identities

$$\begin{aligned}(A_1-A_2)\mathcal{D}n_{21}^k-2n_{21}^k\mathcal{D}(A_2)&=\mathcal{D}(n_{21}^k(A_1-A_2))-n_{21}^k\mathcal{D}(A_1+A_2)\,,\\(A_1-A_2)\mathcal{D}n_{21}^k+2n_{21}^k\mathcal{D}(A_1)&=\mathcal{D}(n_{21}^k(A_1-A_2))+n_{21}^k\mathcal{D}(A_1+A_2)\,,\end{aligned}\tag{17}$$

will be helpful.

3.1. **A first semi-discrete system.** Suppose $T>0$ and let us discretize the temporal interval $[0,T]$ in the following homogeneous way

$$t_k=k\Delta t\,,\quad k\in\{0,1,\dots,K\}\,,\quad \Delta t:=\frac{T}{K}\,.$$

Then, inspired by [8], we choose the following time-discretization of the continuous problem (9)-(14),

$$\begin{aligned}\frac{n_1(A^{k+1})-n_1^k}{\Delta t}&+\nabla\cdot(n_1^k\nabla(A_1^{k+1}-V_s^{k+1}))+\alpha\,\mathcal{R}\mathrm{e}[\mathcal{D}(n_{21}^k(A_1^{k+1}-A_2^{k+1}))]\\&-\alpha\,\mathcal{R}\mathrm{e}[n_{21}^k\mathcal{D}(A_1^{k+1}+A_2^{k+1}-2V_s^{k+1})]\\&-\frac{2\alpha}{\varepsilon}(A_1^{k+1}-A_2^{k+1})\,\mathcal{I}\mathrm{m}(J_x^{21,k}-iJ_y^{21,k})=0\,,\end{aligned}\tag{18}$$

$$\begin{aligned}\frac{n_2(A^{k+1})-n_2^k}{\Delta t}&+\nabla\cdot(n_2^k\nabla(A_2^{k+1}-V_s^{k+1}))+\alpha\,\mathcal{R}\mathrm{e}[\mathcal{D}(n_{21}^k(A_1^{k+1}-A_2^{k+1}))]\\&+\alpha\,\mathcal{R}\mathrm{e}[n_{21}^k\mathcal{D}(A_1^{k+1}+A_2^{k+1}-2V_s^{k+1})]\\&+\frac{2\alpha}{\varepsilon}(A_1^{k+1}-A_2^{k+1})\,\mathcal{I}\mathrm{m}(J_x^{21,k}-iJ_y^{21,k})=0\,,\end{aligned}\tag{19}$$

$$-\gamma^2\Delta V_s^{k+1}=n_1(A^{k+1})+n_2(A^{k+1})\,,\tag{20}$$

$$H(A^{k+1})\psi_l^{k+1}=\lambda_l^{k+1}\psi_l^{k+1}\,,\tag{21}$$

$$n_1(A^{k+1})=\sum_l e^{-\lambda_l^{k+1}}|\psi_l^{1,k+1}|^2\,,\quad n_2(A^{k+1})=\sum_l e^{-\lambda_l^{k+1}}|\psi_l^{2,k+1}|^2\,.\tag{22}$$

In this scheme one searches for the unknowns (A^{k+1},V_s^{k+1}), given (N^k,J_{21}^k). The main difficulty concerning the solution of this system are the non-local relations (21)-(22). We shall thus construct a mapping $(A,V_s)\in$

$(H^1(\Omega,\mathbb{R}))^3 \mapsto \mathcal{F}(A,V_s) \in \mathbb{R}$ whose unique minimum (A^{k+1},V_s^{k+1}) is the solution of system (18)-(22). Once A^{k+1} and the eigenvalues λ_l^{k+1} respectively eigenvectors ψ_l^{k+1} are known, Eqs. (13)-(14) can be used to compute (N^{k+1},J_{21}^{k+1}) and the process can be repeated. Let us thus introduce the two functionals

$$\mathcal{G} : (L^2(\Omega,\mathbb{R}))^2 \to \mathbb{R}\,, \quad \mathcal{F} : (H^1(\Omega,\mathbb{R}))^3 \to \mathbb{R}\,,$$

defined by

$$\mathcal{G}(A) := \sum_l e^{-\lambda_l(A)}\,, \qquad A \in (L^2(\Omega,\mathbb{R}))^2\,, \tag{23}$$

where $\lambda_l(A)$ are the eigenvalues of the Hamiltonian (5), and

$$\mathcal{F}(A,V_s) = \mathcal{G}(A) + \mathcal{F}_1(A,V_s) + \mathcal{F}_2(A,V_s) + \mathcal{F}_3(A,V_s) + \mathcal{F}_4(A)\,, \tag{24}$$

where

$$\mathcal{F}_1(A,V_s) := \frac{\Delta t}{2}\int_\Omega n_1^k|\nabla(A_1-V_s)|^2\,dx + \frac{\Delta t}{2}\int_\Omega n_2^k|\nabla(A_2-V_s)|^2\,dx\,, \tag{25}$$

$$\mathcal{F}_2(A,V_s) := \frac{\gamma^2}{2}\int_\Omega |\nabla V_s|^2\,dx + (n_1^k, A_1-V_s) + (n_2^k, A_2-V_s)\,, \tag{26}$$

$$\mathcal{F}_3(A,V_s) := \alpha\Delta t\,\mathcal{R}\mathrm{e}\left\{\int_\Omega n_{21}^k(A_1-A_2)\mathcal{D}(A_1+A_2-2V_s)\,dx\right\}\,, \tag{27}$$

$$\mathcal{F}_4(A) := \frac{\alpha\Delta t}{\varepsilon}\,\mathcal{I}\mathrm{m}\left\{\int_\Omega (A_1-A_2)^2(J_x^{21,k}-iJ_y^{21,k})\,dx\right\}\,. \tag{28}$$

The computation of the first and second Gateaux derivative of the functionals (23)-(28) can be found in Appendix B and C, respectively. One can immediately see that a solution (A^{k+1},V_s^{k+1}) of the semi-discrete system (18)-(22) satisfies

$$\mathrm{d}\mathcal{F}(A^{k+1},V_s^{k+1})(\delta A,\delta V_s) = 0\,, \qquad \forall\,(\delta A,\delta V_s) \in (H^1(\Omega,\mathbb{R}))^3\,,$$

and inversely. Thus, it remains to show that $\mathcal{F}$ has a unique extremum (minimum). This can be achieved in two steps, as it is detailed in Appendix C. First we show that, under suitable assumptions, the functional $\mathcal{F}$ is strictly convex. Then it is sufficient to show that $\mathcal{F}$ is coercive to obtain the existence and uniqueness of the extremum (A^{k+1},V_s^{k+1}), solution of the system (18)-(22) (see Appendix C).

3.2. **A second semi-discrete system.** We suggest here an alternative way to discretize in time the quantum drift-diffusion model (9)-(15). It is based on the point of view that one advances the spin densities in time, rather than the chemical potentials. We shall implement an explicit forward Euler

scheme:

$$\begin{aligned}\frac{n_1^{k+1}-n_1^k}{\Delta t} &+ \nabla\cdot(n_1^k\nabla(A_1^k-V_s^k)) + \alpha\,\mathcal{R}\mathrm{e}\{\mathcal{D}(n_{21}^k(A_1^k-A_2^k))\} \\ &- \alpha\,\mathcal{R}\mathrm{e}(n_{21}^k\mathcal{D}(A_1^k+A_2^k-2V_s^k)) - \frac{2\alpha}{\varepsilon}(A_1^k-A_2^k)\,\mathcal{I}\mathrm{m}(J_{21}^{x,k}-iJ_{21}^{y,k}) \\ &= 0\,,\end{aligned} \tag{29}$$

$$\begin{aligned}\frac{n_2^{k+1}-n_2^k}{\Delta t} &+ \nabla\cdot(n_2^k\nabla(A_2^k-V_s^k)) + \alpha\,\mathcal{R}\mathrm{e}\{\mathcal{D}[n_{21}^k(A_1^k-A_2^k)]\} \\ &+ \alpha\,\mathcal{R}\mathrm{e}[n_{21}^k\mathcal{D}(A_1^k+A_2^k-2V_s^k)] + \frac{2\alpha}{\varepsilon}(A_1^k-A_2^k)\,\mathcal{I}\mathrm{m}(J_{21}^{x,k}-iJ_{21}^{y,k}) \\ &= 0\,,\end{aligned} \tag{30}$$

$$-\gamma^2\Delta V_s^k = n_1^k + n_2^k\,, \tag{31}$$

$$H(A^k)\psi_l^k = \lambda_l^k\psi_l^k\,, \tag{32}$$

$$N = \sum_l e^{-\lambda_l^k}\begin{pmatrix} |\psi_l^{1,k}|^2 & \psi_l^{1,k}\,\overline{\psi_l^{2,k}} \\ \psi_l^{2,k}\,\overline{\psi_l^{1,k}} & |\psi_l^{2,k}|^2 \end{pmatrix}, \tag{33}$$

$$J_{21}^k = -\frac{i\varepsilon}{2}\sum_l e^{-\lambda_l^k}\left(\overline{\psi_l^{1,k}}\nabla\psi_l^{2,k} - \psi_l^{2,k}\nabla\overline{\psi_l^{1,k}}\right). \tag{34}$$

In this case, given the spin-densities (n_1^k, n_2^k), one first uses the Poisson equation (31) to get V_s^k, then inverts the relations (32)-(33) in order to get the chemical potentials (A_1^k, A_2^k). Finally one advances in time, using the drift-diffusion equations (29)-(30) in order to get the new spin densities (n_1^{k+1}, n_2^{k+1}), and then one repeats the steps. The inversion of the non-local relation (32)-(33) can be achieved by minimizing the functional $\mathcal{G}_n : (L^2(\Omega,\mathbb{R}))^2 \to \mathbb{R}$, defined by

$$\mathcal{G}_n(A) := \mathcal{G}(A) + \int_\Omega n_1^k A_1\,dx + \int_\Omega n_2^k A_2\,dx \tag{35}$$

Indeed, the first derivative of this functional reads

$$\begin{aligned}\mathrm{d}\mathcal{G}_n(A)(\delta A) = &-\sum_l e^{-\lambda_l(A)}\int_\Omega \left(|\psi_l^1(A)|^2\delta A_1 + |\psi_l^2(A)|^2\delta A_2\right)\,dx \\ &+ \int_\Omega n_1^k\delta A_1\,dx + \int_\Omega n_2^k\delta A_2\,dx\,,\end{aligned} \tag{36}$$

which clearly implies that its zeros are solutions of (32)-(33). As shown in Appendix B, the functional $\mathcal{G}_n$ is strictly convex and coercive, admitting hence a unique extremum.

Remark 1. *The two semi-discrete systems presented in this section conserve the total mass* $(n_1 + n_2)$ *because of the particular choice of Dirichlet boundary conditions for the eigenvectors* ψ_l *of the Hamiltonian* (5)*. This can be obtained by integrating the sum of the semi-discrete drift-diffusion equations for* n_1 *and* n_2*, Eqs.* (18)-(19) *or* (29)-(30)*, respectively, over the domain* Ω*. The remaining boundary term is of the form*

$$\int_{\partial\Omega} n_{21}(A_1 - A_2)(1, -i) \cdot \nu(x)\, d\sigma\,,$$

which does not vanish for Neumann boundary conditions. This is in accordance with the remark at the end of Section 2, where we showed that Neumann conditions for ψ_l *lead to a non-hermitian Hamiltonian* (5) *in* $(L^2(\Omega))^2$*.*

4. Fully discrete system

This section is devoted to the full discretization of the continuous spin QDD model (9)-(15). The time discretization was done in the previous section, now we focus on the space discretization. Let $x \in \Omega = [0,1] \times [0,1]$ with the discretization

$$x_{ij} = (\,(j-1)\Delta x\,,\,(i-1)\Delta y\,)\,, \quad j \in \{1,2,\ldots,M\}\,, \quad i \in \{1,2,\ldots,N\}\,,$$
$$\Delta x := \frac{1}{M-1}\,, \qquad \Delta y := \frac{1}{N-1}\,.$$

For functions $f(x)$ on Ω we write $f(x_{ij}) = f_{ij}$. A function $f(x)$ that is subject to homogenous Dirichlet boundary conditions on $\partial\Omega$ satisfies

$$f_{1j} = f_{Nj} = 0 \quad \forall\, j \in \{1,2,\ldots,M\}\,, \quad f_{i1} = f_{iM} = 0 \quad \forall\, i \in \{1,2,\ldots,N\}\,.$$

We introduce the following index transformation,

$$(i,j) \mapsto p \qquad \forall \quad i \in \{2,\ldots,N-1\}\,,\ j \in \{2,\ldots,M-1\}\,,$$

defined by

$$p = (N-2)(j-2) + i - 1\,, \quad p = 1,\ldots,P\,, \qquad P := (N-2)(M-2)\,.$$

For discrete functions $(f_{ij})_{i,j=2}^{N-1,M-1}$ in Ω the following vector notation will be implemented:

$$\hat{f} := (f_p)_{p=1}^{P} \in \mathbb{C}^P\,. \tag{37}$$

The corresponding euclidean scalar product is denoted by

$$(\hat{f}, \hat{g})_P = \Delta x \Delta y \sum_p f_p \overline{g}_p = \Delta x \Delta y \sum_{i=2}^{N-1} \sum_{j=2}^{M-1} f_{ij} \overline{g}_{ij}\,.$$

4.1. **A first fully discrete system (scheme 1).** The discretization matrices $D_x^{\pm}$, $D_y^{\pm}$, D_x, D_y, $\tilde{D}_x$, $\tilde{D}_y$ and Δ_{dir}, used in the following, are defined in Appendix D. In view of the boundary conditions (15), we choose the following space discretization of the semi-discrete system (18)-(22),

$$\begin{aligned}
&\frac{\hat{n}_1(\hat{A}_1^{k+1},\hat{A}_2^{k+1})-\hat{n}_1^k}{\Delta t}-\frac{2\alpha}{\varepsilon}(\hat{A}_1^{k+1}-\hat{A}_2^{k+1})\circ\mathcal{I}\mathrm{m}(\hat{J}_x^{21,k}-i\hat{J}_y^{21,k}) \qquad (38)\\
&-\frac{1}{2}(D_x^+)^T[\hat{n}_1^k\circ D_x^+(\hat{A}_1^{k+1}-\hat{V}_s^{k+1})]-\frac{1}{2}(D_x^-)^T[\hat{n}_1^k\circ D_x^-(\hat{A}_1^{k+1}-\hat{V}_s^{k+1})]\\
&-\frac{1}{2}(D_y^+)^T[\hat{n}_1^k\circ D_y^+(\hat{A}_1^{k+1}-\hat{V}_s^{k+1})]-\frac{1}{2}(D_y^-)^T[\hat{n}_1^k\circ D_y^-(\hat{A}_1^{k+1}-\hat{V}_s^{k+1})]\\
&-\alpha\,\mathcal{R}\mathrm{e}\left\{\widetilde{D}_x^T[\hat{n}_{21}^k\circ(\hat{A}_1^{k+1}-\hat{A}_2^{k+1})]\right\}+\alpha\,\mathcal{R}\mathrm{e}\left\{i\widetilde{D}_y^T[\hat{n}_{21}^k\circ(\hat{A}_1^{k+1}-\hat{A}_2^{k+1})]\right\}\\
&-\alpha\,\mathcal{R}\mathrm{e}\left\{\hat{n}_{21}^k\circ[\widetilde{D}_x(\hat{A}_1^{k+1}+\hat{A}_2^{k+1}-2\hat{V}_s^{k+1})]\right\}\\
&+\alpha\,\mathcal{R}\mathrm{e}\left\{i\hat{n}_{21}^k\circ[\widetilde{D}_y(\hat{A}_1^{k+1}+\hat{A}_2^{k+1}-2\hat{V}_s^{k+1})]\right\}=0\,,
\end{aligned}$$

$$\begin{aligned}
&\frac{\hat{n}_2(\hat{A}_1^{k+1},\hat{A}_2^{k+1})-\hat{n}_2^k}{\Delta t}+\frac{2\alpha}{\varepsilon}(\hat{A}_1^{k+1}-\hat{A}_2^{k+1})\circ\mathcal{I}\mathrm{m}(\hat{J}_x^{21,k}-i\hat{J}_y^{21,k}) \qquad (39)\\
&-\frac{1}{2}(D_x^+)^T[\hat{n}_2^k\circ D_x^+(\hat{A}_2^{k+1}-\hat{V}_s^{k+1})]-\frac{1}{2}(D_x^-)^T[\hat{n}_2^k\circ D_x^-(\hat{A}_2^{k+1}-\hat{V}_s^{k+1})]\\
&-\frac{1}{2}(D_y^+)^T[\hat{n}_2^k\circ D_y^+(\hat{A}_2^{k+1}-\hat{V}_s^{k+1})]-\frac{1}{2}(D_y^-)^T[\hat{n}_2^k\circ D_y^-(\hat{A}_2^{k+1}-\hat{V}_s^{k+1})]\\
&-\alpha\,\mathcal{R}\mathrm{e}\left\{\widetilde{D}_x^T[\hat{n}_{21}^k\circ(\hat{A}_1^{k+1}-\hat{A}_2^{k+1})]\right\}+\alpha\,\mathcal{R}\mathrm{e}\left\{i\widetilde{D}_y^T[\hat{n}_{21}^k\circ(\hat{A}_1^{k+1}-\hat{A}_2^{k+1})]\right\}\\
&+\alpha\,\mathcal{R}\mathrm{e}\left\{\hat{n}_{21}^k\circ[\widetilde{D}_x(\hat{A}_1^{k+1}+\hat{A}_2^{k+1}-2\hat{V}_s^{k+1})]\right\}\\
&-\alpha\,\mathcal{R}\mathrm{e}\left\{i\hat{n}_{21}^k\circ[\widetilde{D}_y(\hat{A}_1^{k+1}+\hat{A}_2^{k+1}-2\hat{V}_s^{k+1})]\right\}=0\,,
\end{aligned}$$

$$-\gamma^2\Delta_{dir}\hat{V}_s^{k+1}=\hat{n}_1(\hat{A}_1^{k+1},\hat{A}_2^{k+1})+\hat{n}_2(\hat{A}_1^{k+1},\hat{A}_2^{k+1})\,, \qquad (40)$$

$$H(\hat{A}_1^{k+1},\hat{A}_2^{k+1})\begin{pmatrix}\hat{\psi}_l^{1,k+1}\\ \hat{\psi}_l^{2,k+1}\end{pmatrix}=\lambda_l^{k+1}\begin{pmatrix}\hat{\psi}_l^{1,k+1}\\ \hat{\psi}_l^{2,k+1}\end{pmatrix}\,, \qquad (41)$$

$$\hat{n}_1(\hat{A}_1^{k+1}, \hat{A}_2^{k+1}) = \sum_l e^{-\lambda_l^{k+1}} \hat{\psi}_l^{1,k+1} \circ \overline{\hat{\psi}_l^{1,k+1}}\,, \tag{42}$$

$$\hat{n}_2(\hat{A}_1^{k+1}, \hat{A}_2^{k+1}) = \sum_l e^{-\lambda_l^{k+1}} \hat{\psi}_l^{2,k+1} \circ \overline{\hat{\psi}_l^{2,k+1}}\,, \tag{43}$$

$$\hat{n}_{21}^{k} = \sum_l e^{-\lambda_l^{k}} \hat{\psi}_l^{2,k} \circ \overline{\hat{\psi}_l^{1,k}}\,, \tag{44}$$

$$\hat{J}_{21}^{x,k} = -\frac{i\varepsilon}{2} \sum_l e^{-\lambda_l^k} \left[D_x(\hat{\psi}_l^{2,k}) \circ \overline{\hat{\psi}_l^{1,k}} - \hat{\psi}_l^{2,k} \circ D_x(\overline{\hat{\psi}_l^{1,k}}) \right], \tag{45}$$

$$\hat{J}_{21}^{y,k} = -\frac{i\varepsilon}{2} \sum_l e^{-\lambda_l^k} \left[D_y(\hat{\psi}_l^{2,k}) \circ \overline{\hat{\psi}_l^{1,k}} - \hat{\psi}_l^{2,k} \circ D_y(\overline{\hat{\psi}_l^{1,k}}) \right]. \tag{46}$$

Here, the operator "$\circ$" symbolizes the component by component multiplication of two vectors in $\mathbb{C}^P$ and the Hamiltonian $H(\hat{A}^{k+1})$ is given by

$$\begin{aligned} &H(\hat{A}_1^{k+1}, \hat{A}_2^{k+1}) = \\ &= \begin{pmatrix} -\frac{\varepsilon^2}{2}\Delta_{dir} + \mathrm{dg}(\hat{V}_{ext,1} + \hat{A}_1^{k+1}) & \varepsilon^2\alpha(D_x - iD_y) \\ -\varepsilon^2\alpha(D_x + iD_y) & -\frac{\varepsilon^2}{2}\Delta_{dir} + \mathrm{dg}(\hat{V}_{ext,2} + \hat{A}_2^{k+1}) \end{pmatrix}, \end{aligned} \tag{47}$$

where $\mathrm{dg}(\hat{f})$ stands for a diagonal $P \times P$ matrix where the diagonal elements are the components f_p of $\hat{f}$. The scheme (38)-(46) is consistent with the continuous model (9)-(15). It is of first order in time and of second order in space. Due to its rather implicit nature, the scheme (38)-(46) is not subjected to any stability condition. The solution $(\hat{A}_1^{k+1}, \hat{A}_2^{k+1}, \hat{V}_s^{k+1})$ of the system (38)-(46) is the minimizer of the following discrete functional $\widehat{\mathcal{F}}(\hat{A}_1, \hat{A}_2, \hat{V}_s) : \mathbb{R}^{3P} \to \mathbb{R}$,

$$\begin{aligned} \widehat{\mathcal{F}}(\hat{A}_1, \hat{A}_2, \hat{V}_s) :&= \widehat{\mathcal{G}}(\hat{A}_1, \hat{A}_2) + \widehat{\mathcal{F}}_1(\hat{A}_1, \hat{A}_2, \hat{V}_s) + \\ &+ \widehat{\mathcal{F}}_2(\hat{A}_1, \hat{A}_2, \hat{V}_s) + \widehat{\mathcal{F}}_3(\hat{A}_1, \hat{A}_2, \hat{V}_s) + \widehat{\mathcal{F}}_4(\hat{A}_1, \hat{A}_2)\,, \end{aligned} \tag{48}$$

where

$$\widehat{\mathcal{G}}(\hat{A}_1, \hat{A}_2) := \sum_{l=1}^{2P} e^{-\lambda_l(\hat{A}_1, \hat{A}_2)}\,, \tag{49}$$

$$\begin{aligned}\widehat{\mathcal{F}}_1(\hat{A}_1,\hat{A}_2,\hat{V}_s) := \frac{\Delta t}{4}\Big[&(\hat{n}_1^k\circ D_x^+(\hat{A}_1-\hat{V}_s),D_x^+(\hat{A}_1-\hat{V}_s))_P\\ &+(\hat{n}_1^k\circ D_x^-(\hat{A}_1-\hat{V}_s),D_x^-(\hat{A}_1-\hat{V}_s))_P+(\hat{n}_1^k\circ D_y^+(\hat{A}_1-\hat{V}_s),D_y^+(\hat{A}_1-\hat{V}_s))_P\\ &+(\hat{n}_1^k\circ D_y^-(\hat{A}_1-\hat{V}_s),D_y^-(\hat{A}_1-\hat{V}_s))_P+(\hat{n}_2^k\circ D_x^+(\hat{A}_2-\hat{V}_s),D_x^+(\hat{A}_2-\hat{V}_s))_P\\ &+(\hat{n}_2^k\circ D_x^-(\hat{A}_2-\hat{V}_s),D_x^-(\hat{A}_2-\hat{V}_s))_P+(\hat{n}_2^k\circ D_y^+(\hat{A}_2-\hat{V}_s),D_y^+(\hat{A}_2-\hat{V}_s))_P\\ &+(\hat{n}_2^k\circ D_y^-(\hat{A}_2-\hat{V}_s),D_y^-(\hat{A}_2-\hat{V}_s))_P\Big]\,,\end{aligned} \tag{50}$$

$$\begin{aligned}\widehat{\mathcal{F}}_2(\hat{A}_1,\hat{A}_2,\hat{V}_s) :&= (\hat{n}_1^k,\hat{A}_1-\hat{V}_s)_P+(\hat{n}_2^k,\hat{A}_2-\hat{V}_s)_P\\ &+\frac{\gamma^2}{2}\Big[(D_x^b\hat{V}_s,D_x^b\hat{V}_s)_P+(D_y^b\hat{V}_s,D_y^b\hat{V}_s)_P\Big]\\ &+\frac{\Delta y}{\Delta x}\sum_{i=1}^N V_{s,iM}^2+\frac{\Delta x}{\Delta y}\sum_{j=1}^M V_{s,Nj}^2\end{aligned} \tag{51}$$

$$\begin{aligned}\widehat{\mathcal{F}}_3(\hat{A}_1,\hat{A}_2,\hat{V}_s) := \alpha\Delta t\,\mathcal{R}\mathrm{e}\Big[&\Big(\hat{n}_{21}^k\circ(\hat{A}_1-\hat{A}_2),\widetilde{D}_x(\hat{A}_1+\hat{A}_2-2\hat{V}_s)\Big)_P\\ &-i\Big(\hat{n}_{21}^k\circ(\hat{A}_1-\hat{A}_2),\widetilde{D}_y(\hat{A}_1+\hat{A}_2-2\hat{V}_s)\Big)_P\Big]\end{aligned} \tag{52}$$

$$\widehat{\mathcal{F}}_4(\hat{A}_1,\hat{A}_2) := \frac{\alpha\Delta t}{\varepsilon}\,\mathcal{I}\mathrm{m}\left[\Big((\hat{A}_1-\hat{A}_2)\circ(\hat{A}_1-\hat{A}_2),\hat{J}_x^{21,k}-i\hat{J}_y^{21,k}\Big)_P\right]\,, \tag{53}$$

and the further discretization matrices D_x^b and D_y^b are also defined in Appendix D. Using the relation

$$\begin{aligned}-(\hat{V}_s,\Delta_{dir}\hat{V}_s)_P &= (D_x^b\hat{V}_s,D_x^b\hat{V}_s)_P+(D_y^b\hat{V}_s,D_y^b\hat{V}_s)_P\\ &+\frac{\Delta y}{\Delta x}\sum_{i=1}^N V_{s,iM}^2+\frac{\Delta x}{\Delta y}\sum_{j=1}^M V_{s,Nj}^2\,,\end{aligned} \tag{54}$$

it can be readily verified that a solution $(\hat{A}_1^{k+1},\hat{A}_2^{k+1},\hat{V}_s^{k+1})$ of (38)-(46) satisfies

$$\mathrm{d}\widehat{\mathcal{F}}(\hat{A}_1^{k+1},\hat{A}_2^{k+1},\hat{V}_s^{k+1})(\delta\hat{A},\delta\hat{V}_s)=0\qquad\forall\,(\delta\hat{A}_1,\delta\hat{A}_2,\delta\hat{V}_s)\in\mathbb{R}^{3P}\,.$$

4.2. **A second fully discrete system (scheme 2).** We chose the following space discretization of the forward Euler scheme (29)-(34):

$$\frac{\hat{n}_1^{k+1}-\hat{n}_1^k}{\Delta t}-\frac{2\alpha}{\varepsilon}(\hat{A}_1^k-\hat{A}_2^k)\circ\mathcal{I}\mathrm{m}(\hat{J}_x^{21,k}-i\hat{J}_y^{21,k})$$
$$-\frac{1}{2}(D_x^+)^T[\hat{n}_1^k\circ D_x^+(\hat{A}_1^k-\hat{V}_s^k)]-\frac{1}{2}(D_x^-)^T[\hat{n}_1^k\circ D_x^-(\hat{A}_1^k-\hat{V}_s^k)]$$
$$-\frac{1}{2}(D_y^+)^T[\hat{n}_1^k\circ D_y^+(\hat{A}_1^k-\hat{V}_s^k)]-\frac{1}{2}(D_y^-)^T[\hat{n}_1^k\circ D_y^-(\hat{A}_1^k-\hat{V}_s^k)]$$
$$-\alpha\,\mathcal{R}\mathrm{e}\left\{\widetilde{D}_x^T[\hat{n}_{21}^k\circ(\hat{A}_1^k-\hat{A}_2^k)]\right\}+\alpha\,\mathcal{R}\mathrm{e}\left\{i\widetilde{D}_y^T[\hat{n}_{21}^k\circ(\hat{A}_1^k-\hat{A}_2^k)]\right\}$$
$$-\alpha\,\mathcal{R}\mathrm{e}\left\{\hat{n}_{21}^k\circ[\widetilde{D}_x(\hat{A}_1^k+\hat{A}_2^k-2\hat{V}_s^k)]\right\}+\alpha\,\mathcal{R}\mathrm{e}\left\{i\hat{n}_{21}^k\circ[\widetilde{D}_y(\hat{A}_1^k+\hat{A}_2^k-2\hat{V}_s^k)]\right\}$$
$$=0\,, \tag{55}$$

$$\frac{\hat{n}_2^{k+1}-\hat{n}_2^k}{\Delta t}+\frac{2\alpha}{\varepsilon}(\hat{A}_1^k-\hat{A}_2^k)\circ\mathcal{I}\mathrm{m}(\hat{J}_x^{21,k}-i\hat{J}_y^{21,k})$$
$$-\frac{1}{2}(D_x^+)^T[\hat{n}_2^k\circ D_x^+(\hat{A}_2^k-\hat{V}_s^k)]-\frac{1}{2}(D_x^-)^T[\hat{n}_2^k\circ D_x^-(\hat{A}_2^k-\hat{V}_s^k)]$$
$$-\frac{1}{2}(D_y^+)^T[\hat{n}_2^k\circ D_y^+(\hat{A}_2^k-\hat{V}_s^k)]-\frac{1}{2}(D_y^-)^T[\hat{n}_2^k\circ D_y^-(\hat{A}_2^k-\hat{V}_s^k)]$$
$$-\alpha\,\mathcal{R}\mathrm{e}\left\{\widetilde{D}_x^T[\hat{n}_{21}^k\circ(\hat{A}_1^k-\hat{A}_2^k)]\right\}+\alpha\,\mathcal{R}\mathrm{e}\left\{i\widetilde{D}_y^T[\hat{n}_{21}^k\circ(\hat{A}_1^k-\hat{A}_2^k)]\right\}$$
$$+\alpha\,\mathcal{R}\mathrm{e}\left\{\hat{n}_{21}^k\circ[\widetilde{D}_x(\hat{A}_1^k+\hat{A}_2^k-2\hat{V}_s^k)]\right\}-\alpha\,\mathcal{R}\mathrm{e}\left\{i\hat{n}_{21}^k\circ[\widetilde{D}_y(\hat{A}_1^k+\hat{A}_2^k-2\hat{V}_s^k)]\right\}$$
$$=0\,, \tag{56}$$

$$-\gamma^2\Delta_{dir}\hat{V}_s^k=\hat{n}_1^k+\hat{n}_2^k\,, \tag{57}$$

$$H(\hat{A}_1^k,\hat{A}_2^k)\begin{pmatrix}\hat{\psi}_l^{1,k}\\ \hat{\psi}_l^{2,k}\end{pmatrix}=\lambda_l^k\begin{pmatrix}\hat{\psi}_l^{1,k}\\ \hat{\psi}_l^{2,k}\end{pmatrix}, \tag{58}$$

$$\hat{n}_1^k=\sum_l e^{-\lambda_l^k}\hat{\psi}_l^{1,k}\circ\overline{\hat{\psi}_l^{1,k}}\,,\qquad \hat{n}_2^k=\sum_l e^{-\lambda_l^k}\hat{\psi}_l^{2,k}\circ\overline{\hat{\psi}_l^{2,k}}\,, \tag{59}$$

$$\hat{n}_{21}^k=\sum_l e^{-\lambda_l^k}\hat{\psi}_l^{2,k}\circ\overline{\hat{\psi}_l^{1,k}}\,, \tag{60}$$

$$\hat{J}_{21}^{x,k} = -\frac{i\varepsilon}{2}\sum_l e^{-\lambda_l^k}\left[D_x(\hat{\psi}_l^{2,k})\circ\overline{\hat{\psi}_l^{1,k}} - \hat{\psi}_l^{2,k}\circ D_x(\overline{\hat{\psi}_l^{1,k}})\right], \tag{61}$$

$$\hat{J}_{21}^{y,k} = -\frac{i\varepsilon}{2}\sum_l e^{-\lambda_l^k}\left[D_y(\hat{\psi}_l^{2,k})\circ\overline{\hat{\psi}_l^{1,k}} - \hat{\psi}_l^{2,k}\circ D_y(\overline{\hat{\psi}_l^{1,k}})\right]. \tag{62}$$

Here, the Hamiltonian H is the same discrete Hamiltonian (47) as in the first fully discrete scheme. Clearly, the scheme (55)-(62) is consistent with the continuous model (9)-(15). It is of first order in time and of second order in space. A drawback of the explicit nature of the forward Euler scheme (29)-(34) is that its full discretization is not unconditionally stable, as compared to the implicit scheme presented in the previous subsection. Rather, the space-time grid must be chosen in such a way that a CFL condition is fulfilled.

The solution of this scheme requires the inversion of the non-local relation (58)-(59) at each time step. For this let us define the discrete version $\widehat{\mathcal{G}}_n : \mathbb{R}^{2P} \to \mathbb{R}$ of (35),

$$\widehat{\mathcal{G}}_n(\hat{A}_1,\hat{A}_2) := \widehat{\mathcal{G}}(\hat{A}_1,\hat{A}_2) + (\hat{n}_1^k,\hat{A}_1)_P + (\hat{n}_2^k,\hat{A}_2)_P\,. \tag{63}$$

It can be easily verified that the first derivative of this functional is given by

$$\begin{aligned}\mathrm{d}\widehat{\mathcal{G}}_n(\hat{A}_1,\hat{A}_2)(\delta\hat{A}_1,\delta\hat{A}_2) = &\left(-\sum_l e^{-\lambda_l^k}\hat{\psi}_l^{1,k}\circ\overline{\hat{\psi}_l^{1,k}} + \hat{n}_1^k,\delta\hat{A}_1\right)_P \\ &+\left(-\sum_l e^{-\lambda_l^k}\hat{\psi}_l^{2,k}\circ\overline{\hat{\psi}_l^{2,k}} + \hat{n}_2^k,\delta\hat{A}_2\right)_P,\end{aligned} \tag{64}$$

whose zeros are hence the solutions of (58)-(59).

Remark 2. *It should be noted that numerical tests performed in Sec. 5 convinced us that the forward Euler scheme presented in this subsection was better suited for a numerical solution of the spin QDD model than a Lax-Friedrichs scheme. In fact, the latter was found to be unstable in the regarded test cases. This is quite surprising since the Eqs.* (29)-(30) *contain a term of conservative form* $\nabla\cdot(n_j\nabla A_j)$. *Therefore, appropriate discretizations for conservation laws* [11]*, such as Lax-Friedrichs, should be used to ensure numerical stability. Moreover, the forward Euler scheme is unconditionally unstable for (linear) equations in conservative form. An explanation for the observed stability can be given by regarding the Lagrange multipliers* $A_j^\varepsilon = A_j^\varepsilon(n_1,n_2)$ *in the semi-classical limit* $\varepsilon\to 0$. *As described in* [2]*, the correct semi classical expansion reads*

$$A_j^\varepsilon(n_1,n_2) = -\log n_j + \frac{\varepsilon^2}{6}\frac{\Delta\sqrt{n_j}}{\sqrt{n_j}} + \mathcal{O}(\varepsilon^2\alpha^2)\,. \tag{65}$$

Therefore, in the limit $\varepsilon \to 0$, the conservative term reads

$$\nabla \cdot (n_j^\varepsilon \nabla A_j^\varepsilon) \qquad \xrightarrow{\varepsilon \to 0} \qquad -\nabla \cdot (n_j \nabla \log n_j)\,. \tag{66}$$

Hence, for small ε, the Eqs. (29)-(30) *resemble a heat equation or a drift-diffusion equation, respectively, where the diffusive term is written in the non-standard form* (66)*. In this case the forward Euler scheme is stable with respect to a CFL condition of the form $\Delta t \leq d\Delta x^2$ for some constant d.*

4.3. **Initialization of scheme 1.** As was briefly mentioned in Sec. 2, a natural way to initialize the system (38)-(46) would be to start from given initial chemical potentials $\hat{A}_1^0$ and $\hat{A}_2^0$, compute the corresponding spin- and current densities and subsequently begin the iteration. However, from an experimental point of view it is more appealing to start from the initial spin densities $\hat{n}_1^0$ and $\hat{n}_2^0$. The problem in the latter approach is the lack of information about the initial spin-mixing quantities $\hat{n}_{21}^0$, $\hat{J}_{21}^{x,0}$ and $\hat{J}_{21}^{y,0}$, which are not directly related to the spin densities. At $t = t^0$ it is thus necessary to do a half step of scheme 2, which means to minimize the functional (63) in order to obtain the chemical potentials corresponding to the initial spin densities $\hat{n}_1^0$ and $\hat{n}_2^0$. One can then proceed according to scheme 1.

5. Numerical results

This section deals with the numerical study of the two fully discrete schemes which were introduced in the previous section. The developed algorithms were implemented in the Fortran 90 language. Eigenvalue problems were solved using the routine 'zheev.f90' from the Lapack library. The solution of scheme 1, equations (38)-(46), was achieved by minimizing the discrete functional (48) at each time step t_k, $k > 0$. At t_0 the system was initialized as detailed in Subsec. 4.3. Each minimization problem was solved by a conjugate gradient method in the parameter space $\mathbb{R}^{3P}$ (or $\mathbb{R}^{2P}$ for scheme 2, respectively). We denote vectors in the discrete space by capital letters $X \in \mathbb{R}^{3P}$, $X = (\hat{A}_1, \hat{A}_2, \hat{V}_s)$, and by ∇_X we denote the gradient in the discrete space. In what follows the dot '$\cdot$' stands for the usual euclidean scalar product in $\mathbb{R}^{3P}$. In order to find the line minimum of $\nabla_X \widehat{\mathcal{F}} \cdot Y_n$, where Y_n denotes the search direction ($|Y_n| = 1$) during the n-th step of the conjugate gradient scheme, a Newton method was employed. The derivative of $\nabla_X \widehat{\mathcal{F}} \cdot Y_n$ in the direction Y_n was computed numerically with a forward discretization and the small step size $\varepsilon_{NT} = 10^{-3}$,

$$(\nabla_X \widehat{\mathcal{F}}(X) \cdot Y_n)' \approx \frac{\nabla_X \widehat{\mathcal{F}}(X + \varepsilon_{NT} Y_n) \cdot Y_n - \nabla_X \widehat{\mathcal{F}}(X) \cdot Y_n}{\varepsilon_{NT}}\,.$$

The same method was applied to the functional $\widehat{\mathcal{G}}_n$ in scheme 2. The Newton method was considered converged when $|\nabla_X \widehat{\mathcal{F}}(X) \cdot Y_n| < 10^{-10}$. We established two convergence criteria for the conjugate gradient method. On the one hand, we demanded that the total mass was conserved up to a factor 10^{-4}. On the other hand, using the notations $X = (x_i)_{i=1}^{3P}$ and $\nabla_X \widehat{\mathcal{F}} = (\partial_{x_i} \widehat{\mathcal{F}})_{i=1}^{3P}$, we demanded that

$$\max_i |\partial_{x_i} \widehat{\mathcal{F}}| < 10^{-3} .$$

Again, the same criteria were applied for the functional $\widehat{\mathcal{G}}_n$ in scheme 2. The time evolution was assumed to have converged if $|n_{1(2)}^{k+1} - n_{1(2)}^k|/\Delta t$ was less than 10^{-1} at each grid point.

Our aim is to test the developed numerical schemes in a typical transistor geometry, depicted in Fig. 1. We expect to obtain equilibrium charge- and spin-distributions for such a device. The source electrode of the transistor is located in the upper left corner of the domain, being held at a fixed potential-value $V_{ext,S} = 0$. The drain electrode is opposite to the source in the upper right corner with a fixed potential-value $V_{ext,D} = -2.0$. The gate electrode, held at the fixed potential $V_{ext,G} = -3.0$, is centered at $x = 0.5$ at the upper boundary of the domain. The values chosen for the electrode potentials are typical ones for a transistor in the on-state (current flowing between the source and the drain).

The transistor environment described above manifests itself in the two spin-up respectively spin-down external potentials $V_{ext,1}$ and $V_{ext,2}$. Prior to starting our simulations, these potentials were computed from the Laplace equation using a Gauss-Seidel scheme, where the fixed values $V_{ext,S}$, $V_{ext,D}$, $V_{ext,G}$ entered as Dirichlet boundary conditions (Neumann conditions were used at non-electrode portions of the domain boundary). On top of that we added a potential barrier of height 2.0 and thickness 0.1, which is centered at $x = 0.5$, and which exists only for spin-up electrons (index '1'). The barrier was thus added to $V_{ext,1}$ only. The potentials $V_{ext,1} + V_s$ and $V_{ext,2} + V_s$ at the starting time t_0 are depicted in Fig. 1.

Once the starting potentials $V_{ext,1}$ and $V_{ext,2}$ have been determined, we are interested in the evolution of given initial spin distributions n_1^0 and n_2^0 in the prescribed transistor environment. For the initial spin densities we choose two Gaussians centered at $(x, y) = (0.5, 0.5)$,

$$\begin{aligned} n_1^0(x,y) &= \frac{1}{0.12\pi}(1.0 + pol) \exp\left(-\frac{(x-0.5)^2}{0.06} - \frac{(y-0.5)^2}{0.06}\right) , \\ n_2^0(x,y) &= \frac{1}{0.12\pi}(1.0 - pol) \exp\left(-\frac{(x-0.5)^2}{0.06} - \frac{(y-0.5)^2}{0.06}\right) . \end{aligned} \tag{67}$$

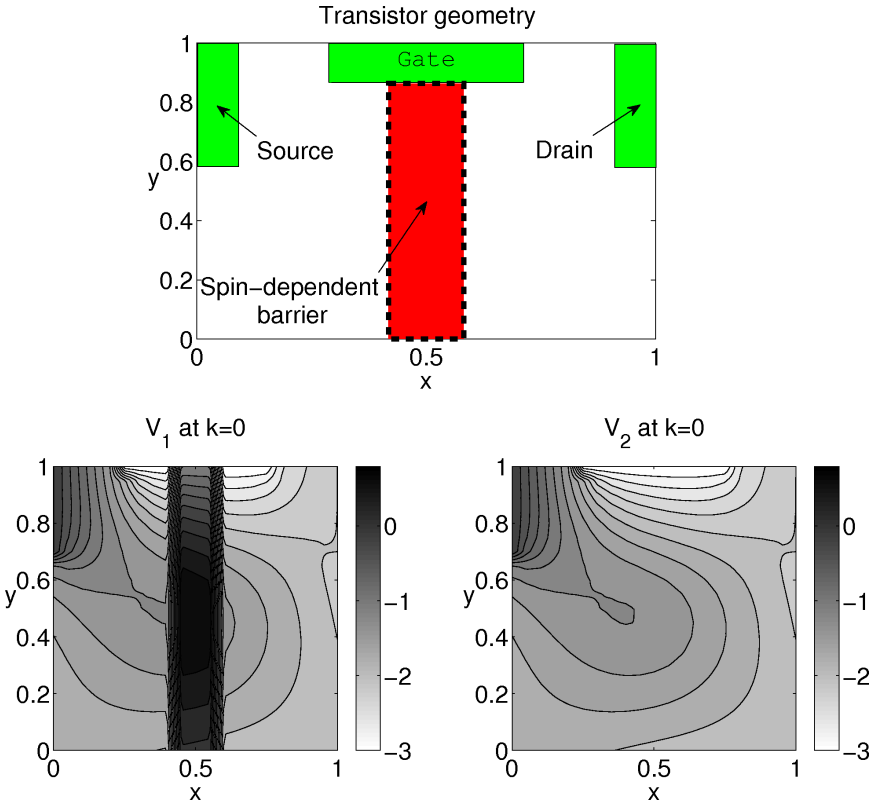

FIGURE 1. Diagram of the transistor geometry used in the simulations and the initial potentials $V_1 = V_{ext,1} + V_s$ and $V_2 = V_{ext,2} + V_s$ in that geometry at $t = t^0$.

Here, *pol* denotes the parameter of the initial spin polarization which was set to $pol = 0.5$. The initial data for n_1 and n_2 were discretized according to the conventions at the beginning of section 4. The initial total mass of the system was 1.0. The parameters of the space-discretization (for scheme 1 and for scheme 2) were chosen as

$$N = 21\,, \quad M = 21\,, \quad \Delta x = 0.05\,, \quad \Delta y = 0.05\,.$$

Employing the initial conditions (67), the numerical solution of scheme 1 and scheme 2, respectively, was carried out for values

$$\alpha = 0.1\,, \qquad \varepsilon = 0.1\,, \tag{68}$$

of the scaled Rashba constant α and the semiclassical parameter ε, respectively. The respective time steps were

$$\text{scheme 1}: \quad \Delta t = 1.0 \times 10^{-2}\,, \quad \text{scheme 2}: \quad \Delta t = 0.5 \times 10^{-4}\,. \tag{69}$$

We note that in scheme 2 the CFL condition imposed a rather small increment on the time discretization.

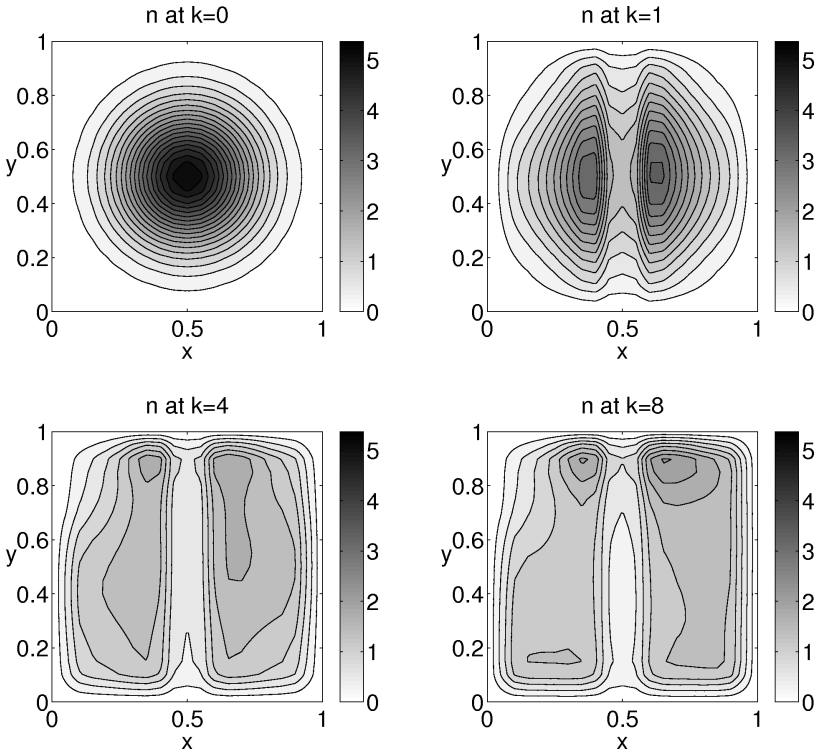

(A) Scheme 1: $\Delta t = 1.0 \times 10^{-2}$.

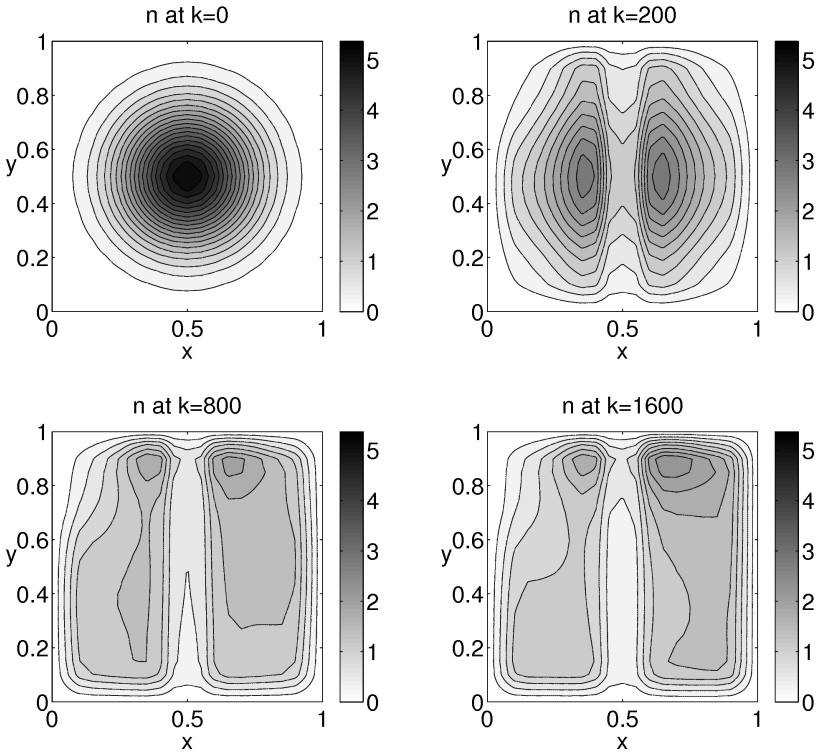

(B) Scheme 2: $\Delta t = 0.5 \times 10^{-4}$.

FIGURE 2. Time evolution of the electron density $n = n_1 + n_2$ in the transistor geometry depicted in Fig. 1.

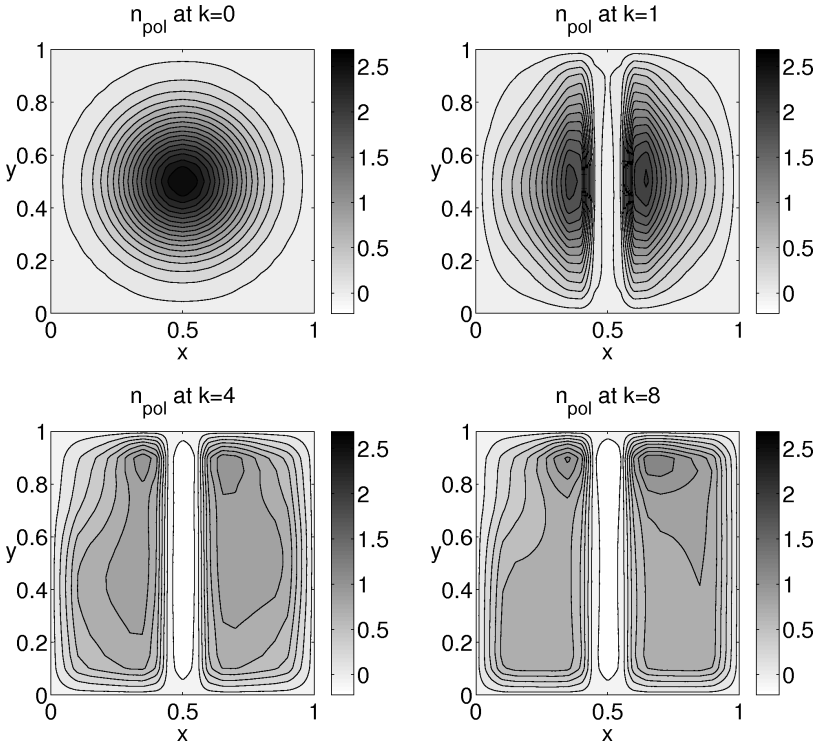

(A) Scheme 1: $\Delta t = 1.0 \times 10^{-2}$.

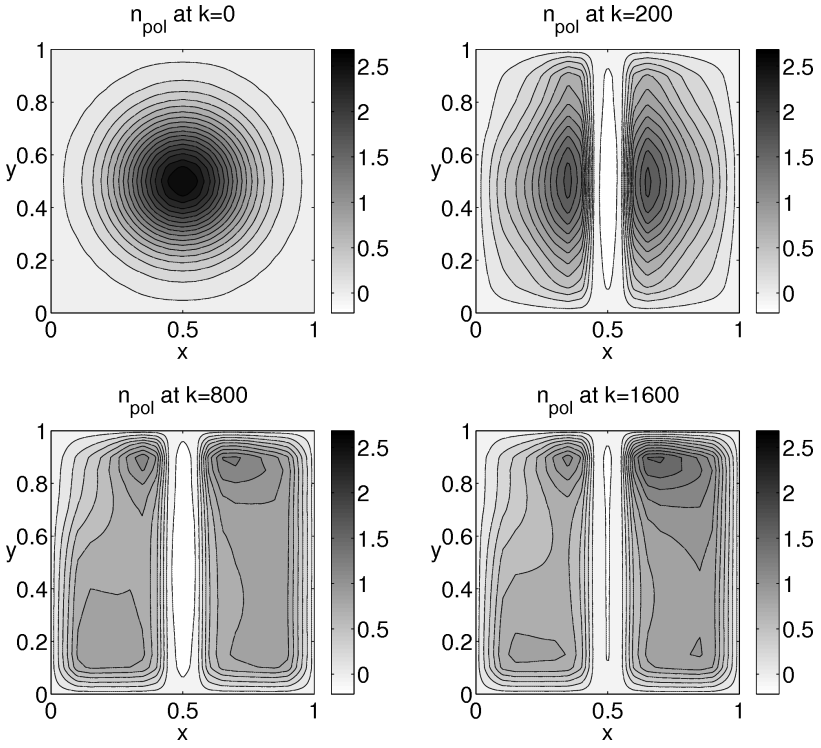

(B) Scheme 2: $\Delta t = 0.5 \times 10^{-4}$.

FIGURE 3. Time evolution of the spin polarization $n_{pol} = n_1 - n_2$ in the transistor geometry depicted in Fig. 1.

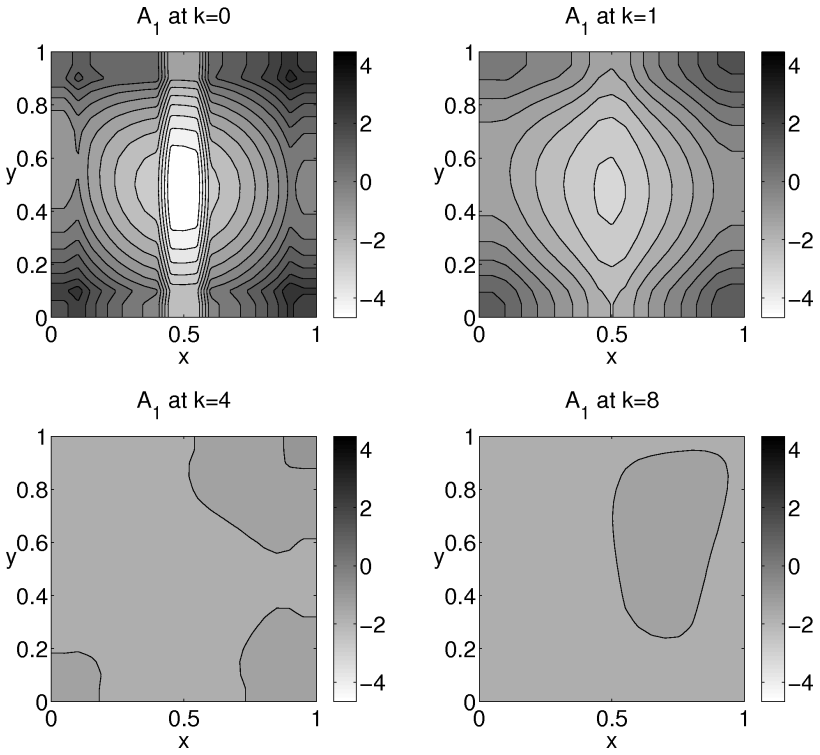

(A) Scheme 1: $\Delta t = 1.0 \times 10^{-2}$.

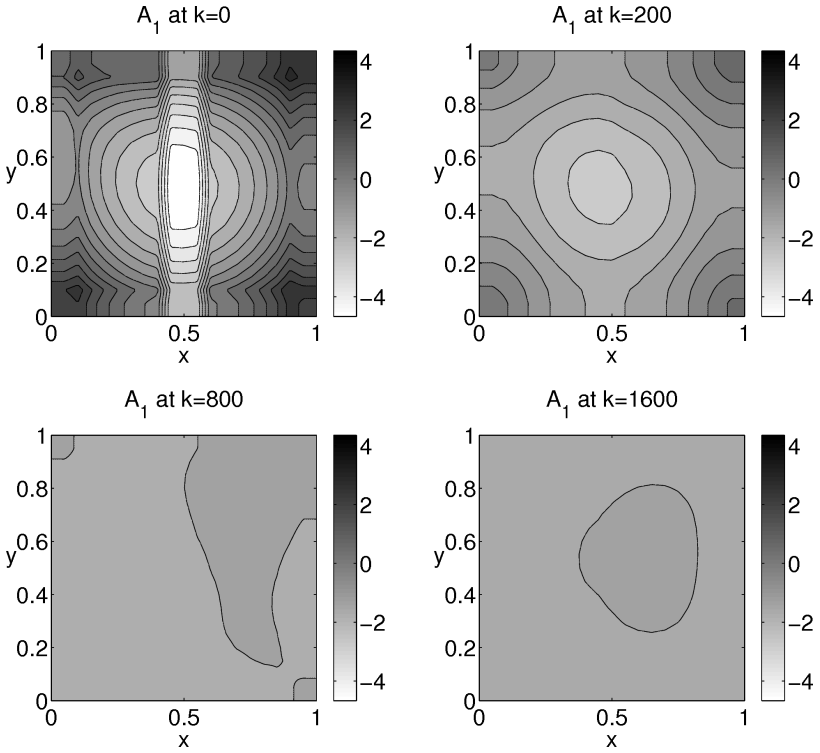

(B) Scheme 2: $\Delta t = 0.5 \times 10^{-4}$.

FIGURE 4. Time evolution of the chemical potential A_1 in the transistor geometry depicted in Fig. 1.

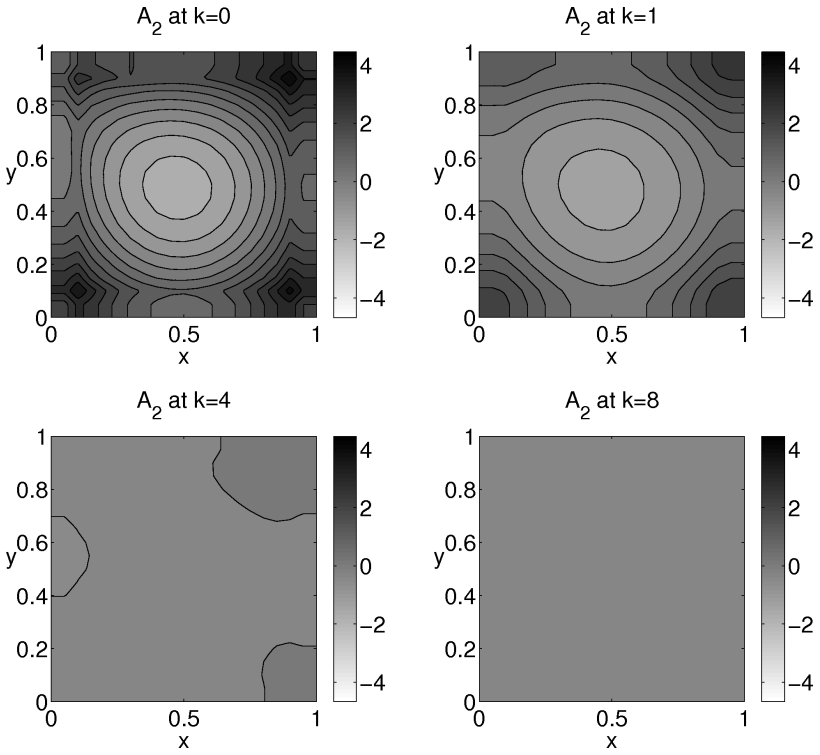

(A) Scheme 1: $\Delta t = 1.0 \times 10^{-2}$.

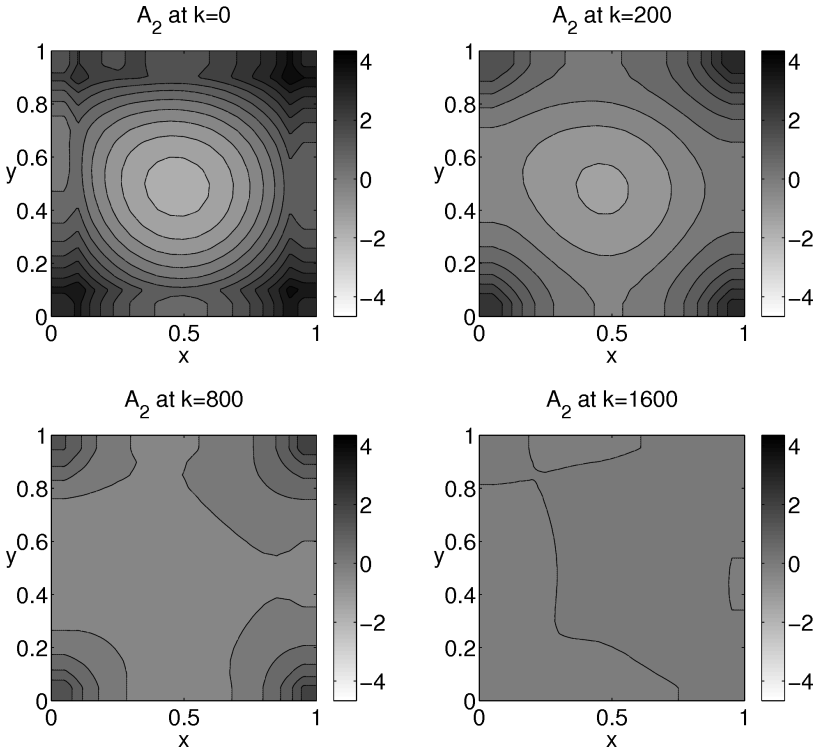

(B) Scheme 2: $\Delta t = 0.5 \times 10^{-4}$.

FIGURE 5. Time evolution of the chemical potential A_2 in the transistor geometry depicted in Fig. 1.

The simulated time evolution of the spin density $n = n_1 + n_2$, the spin polarization $n_{pol} = n_1 - n_2$, the chemical potential A_1 and the chemical potential A_2 are depicted in Figs. 2-5 (all plotted data was interpolated to a grid of 128×128 points using the MATLAB routine "interp2.m"). In each of these Figures the results obtained from scheme 1 are compared with those obtained from scheme 2 during a time span of 8.0×10^{-2}. Let us briefly explain what is observed, starting with the evolution of the electron density $n = n_1 + n_2$ depicted in Fig. 2. At $k = 0$ one identifies the initial Gaussian, given by (67), which, as time evolves, is gradually split into two parts because of the potential barrier located at the center of the transistor, c.f. Figure 1. As one approaches the steady-state (at $k = 8$ for scheme 1 and $k = 1600$ for scheme 2) the electron density has its maximum in the vicinity of the gate and the drain electrode, which is the region where the electron potential $V_{ext} + V_s$ has its lowest value. The region where the potential barrier is located shows a reduced electron density. This can be attributed to the positive barrier height "seen" by spin-up electrons, which impedes these electrons from entering (crossing) this region. Spin-down electrons are much less affected by the barrier, which becomes more transparent when regarding Figs. 4 and 5 for the respective chemical potentials. A first observation is that gradients of A_1 and of A_2 are gradually reduced when approaching the steady-state. Moreover, one clearly observes the barrier in the Lagrange multipier A_1, while in A_2 it is completely absent. Since each Lagrange multiplier depends non-locally on both spin densities, $A_j = A_j(n_1, n_2)$, one would expect the barrier for the spin-up electrons to have some influence on A_2, which is not observed in Fig. 5. The reason for this is the smallness of the parameters ε and α, c.f. Eq. (68). According to the semi classical expansion (65), for small ε and α the Lagrange multiplier A_j is close to a function of n_j alone.

We now turn to an interpretation of the obtained spin polarization n_{pol}, depicted in Fig. 3. A pattern similar to the one for the spin density evolves; however, n_{pol} becomes negative in the region where the potential barrier is located. This is again due to the positive barrier height, which leads to $n_2 > n_1$ in the respective region.

As far as the performance of the two schemes is concerned, the explicit scheme 2 is to be preferred over the implicit scheme 1. The former has the advantage that the functional (63), which is to be minimized at each time step, is defined on the parameter space $\mathbb{R}^{2P}$, as compared to the parameter space $\mathbb{R}^{3P}$ on which the functional (48) of scheme 1 is defined. Considering that, for each search direction in the conjugate gradient method, one has to

solve around 2-10 eigenvalue problems (by then the Newton method has usually converged), a lower-dimensional parameter space significantly reduces the computational cost. However, the CFL condition on the forward Euler scheme prevents a resolution of the model that is considerably faster than with scheme 1, c.f. the difference in the time steps (69). Both schemes are of order 1 in time. For comparable computational cost, scheme 2 is thus preferred over scheme 1 because of the better accuracy, which explains the (small) differences observed in the Figs. 2-5.

6. Conclusion

In this work have carried out a numerical investigation of the quantum diffusive spin model introduced in Ref. [2] and summarized in equations (9)-(15). We formally proved (under suitable assumptions) the existence and uniqueness of a solution of two time discrete versions of this model, on the basis of a functional argument. Furthermore, finite difference approximations of space derivatives resulted in two fully discrete schemes which were later applied to simulate the time evolution of a Rashba electron gas confined in a bounded domain and under the influence of a prescribed external potential. The first scheme is implicit and advances in time the spin chemical potentials, whereas the second scheme is forward Euler and advances in time the spin-up and spin-down densities, respectively. The second scheme is subjected to a CFL stability condition, which results in the use of a considerably smaller time step as compared to the implicit scheme. Our results show that the quantum drift-diffusion model considered here, can be applied for the numerical study of spin-polarized effects due to Rashba spin-orbit coupling and, thus, appears to benefit the design of novel spintronics applications.

Appendix A. Perturbed eigenvalue problem

This section is devoted to the computation of the derivatives $\mathrm{d}\lambda_l(A)(\delta A)$ and $\mathrm{d}\psi_l(A)(\delta A)$ of the eigenvalues and eigenfunctions, respectively, of the Hamiltonian (5), when a small perturbation δA of the chemical potential A is applied. Let us define

$$\delta H = \begin{pmatrix} \delta A_1 & 0 \\ 0 & \delta A_2 \end{pmatrix}, \tag{70}$$

and start from

$$(H + \delta H)(\psi_l + \mathrm{d}\psi_l) = (\lambda_l + \mathrm{d}\lambda_l)(\psi_l + \mathrm{d}\psi_l) \tag{71}$$

where H denotes the Hamiltonian (5). Using $H\psi_l = \lambda_l \psi_l$ one obtains, up to first order in the variations,

$$H\mathrm{d}\psi_l + \delta H \psi_l = \lambda_l \mathrm{d}\psi_l + \mathrm{d}\lambda_l \psi_l \,. \tag{72}$$

Taking now the scalar product with ψ_k and using the orthonormalitiy of the eigenfunctions,

$$(\psi_k, \psi_l)_{L^2} = \int_\Omega (\psi_k^1 \overline{\psi_l^1} + \psi_k^2 \overline{\psi_l^2})\, dx = \delta_{kl} \,, \tag{73}$$

one obtains

$$(\psi_k, H\mathrm{d}\psi_l)_{L^2} + (\psi_k, \delta H \psi_l)_{L^2} = \lambda_l (\psi_k, \mathrm{d}\psi_l)_{L^2} + \mathrm{d}\lambda_l \delta_{kl} \,. \tag{74}$$

Since H is hermitian we have

$$(\psi_k, H\mathrm{d}\psi_l)_{L^2} = (H\psi_k, \mathrm{d}\psi_l)_{L^2} = \lambda_k (\psi_k, \mathrm{d}\psi_l)_{L^2} \,, \tag{75}$$

and (74) can be written as

$$(\psi_k, \delta H \psi_l)_{L^2} = (\lambda_l - \lambda_k)(\psi_k, \mathrm{d}\psi_l)_{L^2} + \mathrm{d}\lambda_l \delta_{kl} \,. \tag{76}$$

For $l = k$ we obtain

$$\mathrm{d}\lambda_l(A)(\delta A) = (\psi_l, \delta H \psi_l)_{L^2} = \int_\Omega \left(|\psi_l^1(A)|^2 \delta A_1 + |\psi_l^2(A)|^2 \delta A_2 \right) dx \,, \tag{77}$$

and for $l \neq k$, assuming that the spectrum of H is non-degenerate, i.e. $\lambda_l \neq \lambda_k$, for $l \neq k$, one obtains

$$(\psi_k, \mathrm{d}\psi_l)_{L^2} = \frac{(\psi_k, \delta H \psi_l)_{L^2}}{\lambda_l - \lambda_k} \,. \tag{78}$$

Since (78) is the projection of $\mathrm{d}\psi_l$ on the k-th basis vector of the eigenbasis of H we may write

$$\begin{aligned} \mathrm{d}\psi_l(A)(\delta A) &= \sum_{k \neq l} \frac{\psi_k}{\lambda_l - \lambda_k} (\psi_k, \delta H \psi_l)_{L^2} = \\ &= \sum_{k \neq l} \frac{\psi_k(A)}{\lambda_l(A) - \lambda_k(A)} \int_\Omega \left(\psi_k^1(A) \overline{\psi_l^1}(A) \delta A_1 + \psi_k^2(A) \overline{\psi_l^2}(A) \delta A_2 \right) dx \,. \end{aligned} \tag{79}$$

Appendix B. The functionals $\mathcal{G}$ and $\mathcal{G}_n$

This appendix is concerned with the study of the functionals $\mathcal{G} : (H^1(\Omega, \mathbb{R}))^2 \to \mathbb{R}$, introduced in (23), and $\mathcal{G}_n : (H^1(\Omega, \mathbb{R}))^2 \to \mathbb{R}$, introduced in (35). The map $\mathcal{G}$ is Gateaux-derivable and its first and second derivatives in the direction $\delta A = (\delta A_1, \delta A_2)$, read

$$\mathrm{d}\mathcal{G}(A)(\delta A) = -\sum_l e^{-\lambda_l(A)} \int_\Omega \left(|\psi_l^1(A)|^2 \delta A_1 + |\psi_l^2(A)|^2 \delta A_2 \right) dx \,,$$

$$\mathrm{d}^2\mathcal{G}(A)(\delta A) = -\sum_{l,k} \frac{e^{-\lambda_l} - e^{-\lambda_k}}{\lambda_l - \lambda_k} \left(\int_\Omega \psi_k^1 \overline{\psi_l^1}\, \delta A_1\, dx + \int_\Omega \psi_k^2 \overline{\psi_l^2}\, \delta A_2\, dx \right)^2 .$$

Let us present the detailed computation of the second derivative. We have

$$\begin{aligned} \mathrm{d}^2\mathcal{G}(A)(\delta A) = &-2\sum_l e^{-\lambda_l}\int_\Omega \mathcal{R}\mathrm{e}\left(\overline{\psi_l^1}\mathrm{d}\psi_l^1\delta A_1 + \overline{\psi_l^2}\mathrm{d}\psi_l^2\delta A_2\right)\,dx \\ &+\sum_l e^{-\lambda_l}\mathrm{d}\lambda_l\int_\Omega\left(|\psi_l^1|^2\delta A_1 + |\psi_l^2|^2\delta A_2\right)\,dx\,. \end{aligned} \tag{80}$$

Let us define the following integrals,

$$I_1^{kl} := \int_\Omega \psi_k^1\overline{\psi_l^1}\,\delta A_1\,dx \qquad\qquad I_2^{kl} := \int_\Omega \psi_k^2\overline{\psi_l^2}\,\delta A_2\,dx\,. \tag{81}$$

Remark that from (77) one deduces

$$\mathrm{d}\lambda_l = I_1^{ll} + I_2^{ll}\,. \tag{82}$$

Thus, the second line in (80) can be written as

$$\sum_l e^{-\lambda_l}\left(I_1^{ll} + I_2^{ll}\right)^2\,. \tag{83}$$

Moreover, from (79) one obtains

$$\begin{aligned} \mathrm{d}\psi_l^1 &= \sum_{k\neq l}\frac{\psi_k^1}{\lambda_l-\lambda_k}\left(I_1^{kl}+I_2^{kl}\right)\,, \\ \mathrm{d}\psi_l^2 &= \sum_{k\neq l}\frac{\psi_k^2}{\lambda_l-\lambda_k}\left(I_1^{kl}+I_2^{kl}\right)\,, \end{aligned} \tag{84}$$

and therefore we have

$$\int_\Omega\left(\overline{\psi_l^1}\mathrm{d}\psi_l^1\delta A_1 + \overline{\psi_l^2}\mathrm{d}\psi_l^2\delta A_2\right)\,dx = \sum_{k\neq l}\frac{1}{\lambda_l-\lambda_k}\left(I_1^{kl}+I_2^{kl}\right)^2\,. \tag{85}$$

The right-hand-side of the first line in (80) can now be written as

$$-2\sum_l\sum_{k\neq l}\frac{e^{-\lambda_l}}{\lambda_l-\lambda_k}\left(I_1^{kl}+I_2^{kl}\right)^2 = -\sum_{l,k,l\neq k}\frac{e^{-\lambda_l}-e^{-\lambda_k}}{\lambda_l-\lambda_k}\left(I_1^{kl}+I_2^{kl}\right)^2\,. \tag{86}$$

Adding (83) and (86) together and making the convention

$$l=k: \qquad \frac{e^{-\lambda_l}-e^{-\lambda_k}}{\lambda_l-\lambda_k} = -e^{-\lambda_l}\,, \tag{87}$$

the second derivative of $\mathcal{G}(A)$ becomes

$$\mathrm{d}^2\mathcal{G}(A)(\delta A) = -\sum_{l,k}\frac{e^{-\lambda_l}-e^{-\lambda_k}}{\lambda_l-\lambda_k}\left(I_1^{kl}+I_2^{kl}\right)^2\,. \tag{88}$$

As a consequence, the map $\mathcal{G}$ is strictly convex. As far as $\mathcal{G}_n$ is concerned, we formally obtain

$$\begin{aligned} \mathcal{G}_n(A) &= \sum_l e^{-\lambda_l(A)} + \int_\Omega n_1^k A_1\,dx + \int_\Omega n_2^k A_2\,dx \\ &\geq e^{-\lambda_1(A)} + \int_\Omega n_1^k A_1\,dx + \int_\Omega n_2^k A_2\,dx \xrightarrow[||A_1||_{L^2}+||A_2||_{L^2}\to\infty]{} \infty\,, \end{aligned} \tag{89}$$

where $\lambda_1(A)$ stands for the smallest eigenvalue of the Hamiltonian $H(A)$,

$$\lambda_1(A) = \min_{\phi \in (H^1(\Omega))^2} (H(A)\phi, \phi)\,, \qquad ||\phi||_{(L^2(\Omega))^2} = 1\,. \tag{90}$$

We are then let to the conclusion that $\mathcal{G}_n$ is strictly convex (as its second derivatives coincide with those of $\mathcal{G}$) and even coercive.

Appendix C. The functional $\mathcal{F}$

In this appendix we are concerned with the convexity and coercivity of the functional $\mathcal{F}$, given by (25)-(28), in order to show that under some assumptions $\mathcal{F}$ admits a unique minimum. The first and second Gateaux derivative of the functionals (25)-(28) are given by

$$\begin{aligned}
\mathrm{d}\mathcal{F}_1(A,V_s)(\delta A,\delta V_s) =& -\Delta t \int_\Omega \nabla\cdot(n_1^k\nabla(A_1-V_s))(\delta A_1-\delta V_s)\,dx \\
& -\Delta t \int_\Omega \nabla\cdot(n_2^k\nabla(A_2-V_s))(\delta A_2-\delta V_s)\,dx\,,
\end{aligned}$$

$$\begin{aligned}
\mathrm{d}^2\mathcal{F}_1(A,V_s)(\delta A,\delta V_s) =& -\Delta t \int_\Omega \nabla\cdot[n_1^k\nabla(\delta A_1-\delta V_s)](\delta A_1-\delta V_s)\,dx \\
& -\Delta t \int_\Omega \nabla\cdot[n_2^k\nabla(\delta A_2-\delta V_s)](\delta A_2-\delta V_s)\,dx \\
=& \Delta t \int_\Omega n_1^k|\nabla(\delta A_1-\delta V_s)|^2\,dx + \Delta t\int_\Omega n_2^k|\nabla(\delta A_2-\delta V_s)|^2\,dx\,,
\end{aligned}$$

$$\begin{aligned}
\mathrm{d}\mathcal{F}_2(A,V_s)(\delta A,\delta V_s) =& -\gamma^2\int_\Omega \Delta V_s\delta V_s\,dx - \int_\Omega (n_1^k+n_2^k)\delta V_s\,dx \\
& + \int_\Omega n_1^k\delta A_1\,dx + \int_\Omega n_2^k\delta A_2\,dx\,,
\end{aligned}$$

$$\mathrm{d}^2\mathcal{F}_2(A,V_s)(\delta A,\delta V_s) = -\gamma^2\int_\Omega(\Delta\delta V_s)\delta V_s\,dx = \gamma^2\int_\Omega|\nabla\delta V_s|^2\,dx\,,$$

$$\begin{aligned}
\mathrm{d}\mathcal{F}_3(A,V_s)(\delta A,\delta V_s) =& -\alpha\Delta t\,\mathcal{R}\mathrm{e}\left\{\int_\Omega \mathcal{D}[n_{21}^k(A_1-A_2)](\delta A_1+\delta A_2-2\delta V_s)\,dx\right\} \\
& +\alpha\Delta t\,\mathcal{R}\mathrm{e}\left\{\int_\Omega n_{21}^k\mathcal{D}(A_1+A_2-2V_s)(\delta A_1-\delta A_2)\,dx\right\}\,,
\end{aligned}$$

$$\mathrm{d}^2\mathcal{F}_3(A,V_s)(\delta A,\delta V_s) = 2\alpha\Delta t\,\mathcal{R}\mathrm{e}\left\{\int_\Omega n_{21}^k\mathcal{D}(\delta A_1+\delta A_2-2\delta V_s)(\delta A_1-\delta A_2)\,dx\right\}\,,$$

$$\mathrm{d}\mathcal{F}_4(A)(\delta A) = \frac{2\alpha\Delta t}{\varepsilon}\,\mathcal{I}\mathrm{m}\left\{\int_\Omega (A_1-A_2)(\delta A_1-\delta A_2)(J_x^{21,k}-iJ_y^{21,k})\,dx\right\}\,,$$

$$\mathrm{d}^2\mathcal{F}_4(A)(\delta A) = \frac{2\alpha\Delta t}{\varepsilon}\,\mathcal{I}\mathrm{m}\left\{\int_\Omega (\delta A_1-\delta A_2)^2(J_x^{21,k}-iJ_y^{21,k})\,dx\right\}\,.$$

To show that $\mathcal{F}$ is strictly convex, it is sufficient to show that

$$\mathrm{d}^2\mathcal{F}(A,V_s)(\delta A,\delta V_s)\geq 0\,,\quad \forall \delta A,\delta V_s\,.$$

One can see immediatly that the terms corresponding to $\mathcal{G}$, $\mathcal{F}_1$ and $\mathcal{F}_2$ are positive. Nevertheless, nothing can be said about the sign of the terms corresponding to $\mathcal{F}_3$ and $\mathcal{F}_4$. Assuming on the other hand that ε is a small parameter, which is a physical hypothesis, one can incorporate these latter terms in the former ones. Inspired by a formal proof in [2], we may assume that

$$n_{21}^k=\mathcal{O}(\varepsilon^2)\,,\quad \mathcal{I}\mathrm{m}(J_x^{21,k}-iJ_y^{21,k})=2c\varepsilon\alpha\frac{e^{-A_1^k}-e^{-A_2^k}}{A_2^k-A_1^k}+\mathcal{O}(\varepsilon^3)\,,$$

for some constant $c>0$. We remark, then, that the dominant term in $d^2\mathcal{F}_4$,

$$4c\alpha^2\Delta t\left\{\int_\Omega(\delta A_1-\delta A_2)^2\frac{e^{-A_1^k}-e^{-A_2^k}}{A_2^k-A_1^k}\,dx\right\}\,,$$

is positive.
Concerning the coercivity, it is enough to show that

$$|\mathcal{F}(A,V_s)|\xrightarrow[||A||_{H^1}+||V_s||_{H^1}\to\infty]{}\infty\,.$$

In [8] this property has been shown for the first terms $\mathcal{X}:=\mathcal{G}+\mathcal{F}_1+\mathcal{F}_2$, by proving that if $|\mathcal{X}(A,V_s)|<c_1$ for some constant $c_1>0$, than there exists a constant $c_2>0$ such that $||A||_{H^1}+||V_s||_{H^1}<c_2$. We can adapt this result in the present case, by assuming again that ε is a small parameter. Indeed, one can again incorporate the new terms $\mathcal{F}_3+\mathcal{F}_4$ in $\mathcal{X}$, by proving the existence of some constant $C>0$, such that

$$C|\mathcal{X}(A,V_s)|\leq|\mathcal{F}(A,V_s)|\,,$$

which proves coercivity. Thus, the functional $\mathcal{F}$, being strictly convexe and coercive, admits a unique minimum.

Appendix D. Discretization matrices

Let us present here the discretization matrices used for the fully discrete systems (see Section 4). Let $\mathbb{1}$ stands for the $(N-2)\times(N-2)$ identity

matrix. Then we have the following discretization matrices:

$$D_x^+ = \frac{1}{\Delta x}\begin{pmatrix} -\mathbb{1} & \mathbb{1} & & & \\ 0 & -\mathbb{1} & \mathbb{1} & & \\ & \ddots & \ddots & \ddots & \\ & & 0 & -\mathbb{1} & \mathbb{1} \\ & & & 0 & 0 \end{pmatrix} \in \mathbb{R}^{P\times P},$$

$$D_x^- = \frac{1}{\Delta x}\begin{pmatrix} 0 & 0 & & & \\ -\mathbb{1} & \mathbb{1} & 0 & & \\ & \ddots & \ddots & \ddots & \\ & & -\mathbb{1} & \mathbb{1} & 0 \\ & & & -\mathbb{1} & \mathbb{1} \end{pmatrix} \in \mathbb{R}^{P\times P},$$

$$D_y^+ = \frac{1}{\Delta y}\begin{pmatrix} d_y^+ & & \\ & \ddots & \\ & & d_y^+ \end{pmatrix}, \qquad D_y^- = \frac{1}{\Delta y}\begin{pmatrix} d_y^- & & \\ & \ddots & \\ & & d_y^- \end{pmatrix},$$

$$D_y^+, D_y^- \in \mathbb{R}^{P\times P},$$

$$d_y^+ = \begin{pmatrix} -1 & 1 & & & \\ 0 & -1 & 1 & & \\ & \ddots & \ddots & \ddots & \\ & & 0 & -1 & 1 \\ & & & 0 & 0 \end{pmatrix} \in \mathbb{R}^{(N-2)\times(N-2)},$$

$$d_y^- = \begin{pmatrix} 0 & 0 & & & \\ -1 & 1 & 0 & & \\ & \ddots & \ddots & \ddots & \\ & & -1 & 1 & 0 \\ & & & -1 & 1 \end{pmatrix} \in \mathbb{R}^{(N-2)\times(N-2)},$$

$$\widetilde{D}_x = \frac{D_x^+ + D_x^-}{2}, \qquad \widetilde{D}_y = \frac{D_y^+ + D_y^-}{2},$$

$$\Delta_{dir} = \Delta^x + \Delta^y \quad \in \mathbb{R}^{P\times P}\,,$$

$$\Delta^x = \frac{1}{(\Delta x)^2}\begin{pmatrix} -2\mathbb{1} & \mathbb{1} & & & \\ \mathbb{1} & -2\mathbb{1} & \mathbb{1} & & \\ & \ddots & \ddots & \ddots & \\ & & \mathbb{1} & -2\mathbb{1} & \mathbb{1} \\ & & & \mathbb{1} & -2\mathbb{1} \end{pmatrix} \in \mathbb{R}^{P\times P}\,.$$

$$\Delta^y := \frac{1}{(\Delta y)^2}\begin{pmatrix} l_y & & \\ & \ddots & \\ & & l_y \end{pmatrix} \in \mathbb{R}^{P\times P}\,.$$

$$l_y = \begin{pmatrix} -2 & 1 & & & \\ 1 & -2 & 1 & & \\ & \ddots & \ddots & \ddots & \\ & & 1 & -2 & 1 \\ & & & 1 & -2 \end{pmatrix} \in \mathbb{R}^{(N-2)\times(N-2)}\,,$$

$$D_x = \frac{1}{2\Delta x}\begin{pmatrix} 0 & \mathbb{1} & & & \\ -\mathbb{1} & 0 & \mathbb{1} & & \\ & \ddots & \ddots & \ddots & \\ & & -\mathbb{1} & 0 & \mathbb{1} \\ & & & -\mathbb{1} & 0 \end{pmatrix} \in \mathbb{R}^{P\times P}\,,$$

$$D_y := \frac{1}{2\Delta y}\begin{pmatrix} d_y & & \\ & \ddots & \\ & & d_y \end{pmatrix} \in \mathbb{R}^{P\times P}\,.$$

$$d_y = \begin{pmatrix} 0 & 1 & & & \\ -1 & 0 & 1 & & \\ & \ddots & \ddots & \ddots & \\ & & -1 & 0 & 1 \\ & & & -1 & 0 \end{pmatrix} \in \mathbb{R}^{(N-2)\times(N-2)},$$

$$D_x^b = \frac{1}{\Delta x} \begin{pmatrix} \mathbb{1} & 0 & & & \\ -\mathbb{1} & \mathbb{1} & 0 & & \\ & \ddots & \ddots & \ddots & \\ & & -\mathbb{1} & \mathbb{1} & 0 \\ & & & -\mathbb{1} & \mathbb{1} \end{pmatrix} \in \mathbb{R}^{P\times P}.$$

$$D_y^b = \frac{1}{\Delta y} \begin{pmatrix} d_y^b & & \\ & \ddots & \\ & & d_y^b \end{pmatrix} \in \mathbb{R}^{P\times P},$$

$$d_y^b = \begin{pmatrix} 1 & 0 & & & \\ -1 & 1 & 0 & & \\ & \ddots & \ddots & \ddots & \\ & & -1 & 1 & 0 \\ & & & -1 & 1 \end{pmatrix} \in \mathbb{R}^{(N-2)\times(N-2)},$$

Acknowledgments. This work has been supported by the ANR project QUATRAIN and by the french-italian research project GREFI-MEFI. S. Possanner acknowledges the support from the Austrian Science Fund, Vienna, under the contract number P21326-N16. L. Barletti acknowledges support from the Italian National Project (PRIN) *Mathematical problems of kinetic theories and applications*, prot. 2009NAPTJF 003.

References

[1] M. Ancona, *Diffusion-drift modeling of strong inversion layers,* COMPEL **6**, 11–18 (1987).

[2] L. Barletti and F. Méhats, *Quantum drift-diffusion modeling of spin transport in nanostructures,* J. Math. Phys. **51**, 053304(20) (2010).

[3] Y. Bychkov, and E. I. Rashba, *Properties of a 2D electron gas with lifted spectral degeneracy,* JETP Letters **39**(2), 78–81 (1984).

[4] P. Degond, S. Gallego and F. Méhats, *An entropic quantum drift-diffusion model for electron transport in resonant tunneling diodes,* J. Comput. Phys. **221**, 226–249 (2007).

[5] P. Degond, F. Méhats and C. Ringhofer, *Quantum energy-transport and drift-diffusion models,* J. Stat. Phys. **118**(3-4), 625–667 (2005).

[6] P. Degond and C. Ringhofer, *Quantum moment hydrodynamics and the entropy principle,* J. Stat. Phys. **112**(3-4), 587–628 (2003).

[7] B. Derrida, J. Lebowitz, E. Speer and H. Spohn, *Fluctuations of a stationary nonequilibrium interface,* Phys. Rev. Letters **67**, 165–168 (1991).

[8] S. Gallego and F. Méhats, *Entropic discretization of a quantum drift-diffusion model,* SIAM J. Numer. Anal. **43**(5), 1828–1849 (2006).

[9] R. El Hajj, *Diffusion models for spin transport derived from the spinor Boltzmann equation,* Comm. Math. Sci. (to appear).

[10] A. Jüngel, *Transport equations for semiconductors,* Springer, Berlin, 2009.

[11] R. LeVeque, *Numerical Methods for Conservation Laws,* Second Edition, Birkhäuser, Basel-Boston-Berlin, 1992.

[12] P. Markowich, C. Ringhofer and C. Schmeiser, *Semiconductor equations,* Springer, Vienna, 1990.

[13] F. Méhats and O. Pinaud, *A*n inverse problem in quantum statistical physics, J. Stat. Phys. **140**, 565–602 (2010)

[14] F. Méhats and O. Pinaud, *A* problem of moment realizability in quantum statistical physics, Kinet. Relat. Models **4**(4), 1143–1158 (2011)

[15] S. Possanner and C. Negulescu, *Diffusion limit of a generalized matrix Boltzmann equation for spin-polarized transport,* Kinet. Relat. Models **4**(4), 1159–1191 (2011).

[16] F. Poupaud, *Diffusion approximation of the linear semiconductor Boltzmann equation: analysis of boundary layers,* Asympt. Anal. **4**, 293–317 (1991).

[17] W. van Roosbroeck, *Theory of flow of electrons and holes in germanium and other semiconductors,* Bell Syst. Techn. J. **29**, 560–607 (1950).

[18] S. Saikin, *Drift-diffusion model for spin-polarized transport in a non-degenerate 2DEG controlled by spin-orbit interaction,* J. Phys.: Condens. Matter **16**, 5071–5081 (2004).

[19] I. Žutić, J. Fabian and S. Das Sarma, *Spintronics: fundamentals and applications,* Rev. Mod. Phys, **76**(2), 323–410 (2002).

Dipartimento di Matematica, Università di Firenze, Italia
E-mail address: barletti@math.unifi.it

INRIA IPSO Team, IRMAR, Université de Rennes 1, France
E-mail address: florian.mehats@univ-rennes1.fr

IMT, Université Paul Sabatier, Toulouse, France
E-mail address: claudia.negulescu@math.univ-toulouse.fr

IMT, Université Paul Sabatier, Toulouse, France
E-mail address: Stefan.Possanner@math.univ-toulouse.fr